THE FADDEEV APPROACH TO HIGH ENERGY ATOMIC COLLISIONS
AND THE SIGNIFICANCE OF CORRESPONDENCE IDENTITIES.

by

NEIL HUTTON, B.Sc.

Thesis submitted to the University of Stirling
for the degree of Doctor of Philosophy.

Physics Department
University of Stirling
STIRLING,
November, 1973.

ABSTRACT

The Faddeev equations enable one to express the
scattering amplitude for a three-body process
interacting via binary potentials in terms of the
two-body off-shell Coulomb T matrices. In the
first order iterate the equations reduce to a sum
of two terms. A form of the two-body off-shell
Coulomb T matrix is presented which can be
expressed partially as a sum over the classical
trajectories of the scattering particles. It is
shown that in the limit of high energies and
non-zero scattering angles an on-shell correspondence
identity exists for this T matrix, so that only
the classical path term contributes to the
scattering amplitude.

The classical path approximation is applied to
elastic and inelastic collisions of electrons on
hydrogen atoms. For elastic collisions the first
order Faddeev approximation predicts differential
cross sections considerably larger than those
predicted by the first Born approximation at
energies where the Born approximation is expected
to be good. At angles of scattering above 30°
our results are identical to those calculated using
a different exact form of the Coulomb T matrix
(Chen and Sinfailam, 1972). In the Faddeev

approximation the differential cross section diverges
at small angles of scattering. The angular and
energy distributions of the differential cross
section for inelastic collisions are close to the
predictions of the Coulomb projected Born approximation
(Geltman and Hidalgo, 1971), though the latter
approximation predicts much smaller cross sections.
Singularities in the on-shell Coulomb T matrix
associated with the long range nature of the
Coulomb potential are responsible for both the
zero angle divergence and the overestimation of
the differential cross section in the Faddeev
approximation.

In conclusion we comment on the importance of recent
calculations of the second-order iterate of the
Faddeev equations for electron-hydrogen scattering
(Chen et.al., 1973) where it is shown that the
differential cross section for elastic scattering
approaches the Born result. This demonstrates that
cancellation occurs between the singularities in
the first-order and second-order terms of the
Faddeev equations.

ACKNOWLEDGEMENTS

This analysis of the two-body off-shell Coulomb T
matrix was initiated by Dr. M.J. Roberts. I
should like to thank him for the sound supervision
and advice which was always made readily available
during this research project. I should like to
thank my colleagues in the Physics Department at
Stirling, many of whom at one time or another
helped my understanding of atomic physics. In
particular Professor I.C. Percival and Dr. D. Banks
made inspiring comments on my research topic, and the
latter gave invaluable assistance with numerical
calculations. I am grateful to Professor J.C.Y. Chen
of the University of California for enlightening
conversations and for providing me with copies of
his work in advance of publication.

During the period of research I was financially
aided by the Science Research Council to which I
am grateful.

CONTENTS

CHAPTER 1

PRELIMINARIES

1.1 Introduction

The theoretical study of electron atom collisions
has attracted physicists for over half a century
(for a detailed review see Mott and Massey). In
many instances the studies have been limited to one
of the simplest atomic collision processes, namely
the scattering of electrons by atomic hydrogen. This
process is a three-body collision involving a system
which initially consists of an incident electron and
a bound electron and proton pair. An exact solution
of the three-body problem has long eluded physicists,
however recent work by Faddeev (1961, 1963, 1965, 1970)
led to a more rigorous analysis of the problem than
hitherto. Chen and Joachain (1971) have shown that
Faddeev's analysis for three bodies is equivalent to
a symmetric version of the Watson multiple-scattering
theory (Goldberger and Watson, p.749).

Earlier calculations on the collision process, both
quantal and classical, had met with limited success.
An extreme paucity of absolute experimental
measurements of the differential and total cross
sections for electron hydrogen collisions had made
interpretation of theoretical results difficult. It

is not the purpose of this thesis to formulate a
classical description of the scattering process,
though correspondence identities between quantum
mechanical results obtained and classical concepts
will be emphasised, so we refer the reader to a
review by Burgess and Percival (1963) for developments
in classical scattering theory.

In quantum mechanical calculations the approximation
used depends mainly on the energy at which the
collision takes place. For low energy collisions
much scattering data has been obtained from applications
of the close coupling and related methods (see for
instance, Burke and Seaton, 1971). We shall be more
interested in the scattering of electrons by hydrogen
atoms at high energies, where the most common
approximation used is that of Born (1926). This
method is briefly described in operator notation
below.

1.2 Scattering cross sections and the Born approximation

The quantities of most interest to us in collision
theory are cross sections. The differential cross
section, $d\sigma/d\Omega$, is defined as the intensity of
scattered particles per unit solid angle per unit
flux, measured at large distances from the scattering
interaction itself. The differential cross section
for the scattering of a particle by a bound pair
interacting via a potential V is (Messiah, ps.306,
335).

$$\frac{d\sigma}{d\Omega} = \frac{\mu^2}{4\pi^2\hbar^4} \left| \langle \phi_F | V | \psi_i^{(+)} \rangle \right|^2 \qquad (1.1)$$

where μ is the mass of the incident particle
reduced relative to the centre of mass of the bound
pair. Here, and throughout this thesis, ϕ_F
represents a final state of the system in the absence
of interaction, whereas $\psi_i^{(+)}$ is the initial full
solution of the Schrödinger equation determined by
the boundary conditions related to the scattering of
the incident particle. The factor $\left(\mu^2 / 4\pi^2\hbar^4 \right)$
is dependent on the normalisation chosen for the
initial and final states. Expression (1.1) is exact;
the Born approximation expresses $\psi_i^{(+)}$, and thus
$\frac{d\sigma}{d\Omega}$, in increasing powers of the potential V .

The first Born approximation is obtained by replacing
$\psi_i^{(+)}$ with the unperturbed state ϕ_i . Essentially
one says that the potential V is so weak that the
system is unperturbed by the passage of the incident
particle, an approximation which is known to be good
for high energy incident particles (Messiah, p.813).
Successive approximations in the Born expansion are
obtained by using the following expansion for $|\psi_i^{(+)}\rangle$,

$$|\psi_i^{(+)}\rangle = \left(1 + \sum_{N=1}^{\infty} \left[G_o^{(+)}(E) V \right]^N \right) |\phi_i\rangle \qquad (1.2)$$

$G_o^{(+)}(E)$ is the free-wave Green function with outgoing
wave asymptotic behaviour for three non-interacting

particles and total energy E . We will find it useful to express the second term in Equation (1.2) in terms of the outgoing scattered wave Green function $G^{(+)}(E)$ (Messiah, p.823)

$$\sum_{N=1}^{\infty} \left[G_o^{(+)}(E) \, V \right]^N = G^{(+)}(E) \, V \qquad (1.3)$$

The ability of the Born expansion method to give a value of $d\sigma/d\Omega$ close to the exact value, depends on the convergence of the expansion (1.2). Whilst the Born series has been shown to converge quickly at high energies for the potential scattering of a particle (Zemach and Klein, 1958), the convergence properties for complex collisions are not well understood. For three-body collisions, Newton (p.557) has shown that δ-functions occur in the analysis which make the integral kernels for the Born expansion badly behaved. In particular for the case of rearrangement collisions Aaron et.al. (1961) have suggested that the Born series is divergent, though we note that this claim has been refuted by Dettmann and Leibfried (1968). This scepticism about the convergence properties of the Born expansion led to a new formulation of Equation (1.1) in terms of the T operator, and to the more detailed analysis of Faddeev.

1.3 The T Operator and the Faddeev Equations

The T operator is defined in matrix representation by its elements

$$T_{if} = \langle \phi_f | T | \phi_i \rangle = \langle \phi_f | V | \psi_i^{(+)} \rangle \qquad (1.4)$$

The first Born approximation to the T matrix is thus

$$T_{if}^B = \langle \phi_f | V | \phi_i \rangle \qquad (1.5)$$

We can define the differential cross section directly in terms of the T matrix from Equation (1.1)

$$\frac{d\sigma}{d\Omega} = \frac{\mu^2}{4\pi^2 \hbar^4} |T_{if}|^2 \qquad (1.6)$$

In this formalism the matrix elements are taken between free state wave functions which can be written down exactly for the problems we are to consider.

Using Equations (1.2) - (1.4) we can obtain, using simple operator algebra, the following formal expressions for the three-body T operator

$$T(E) = V + V G^{(+)}(E) V \qquad (1.7a)$$

$$\text{and} \quad T(E) = V + V G_0^{(+)}(E) T(E) \qquad (1.7b)$$

For three particles interacting only via two-body potentials, the interaction potential is given by

$$V = \sum_{i=1}^{3} V_i \qquad (1.8)$$

where V_i represents the two-body interaction between particles j and k. We can then introduce the two-body T operators, T_i $(i = 1, 2, 3)$, which are defined in terms of the two-body free wave Green function $G_o^{(+)}(E)$,

$$T_i(E) = V_i + V_i G_o^{(+)}(E) T_i(E) \qquad (1.9)$$

$T_i(E)$ represents the two-body T matrix for the interaction between particles j and k with particle i as a spectator. We evaluate the matrix elements of $T_i(E)$ between momentum states; that is, $\langle p | T_i(E) | p' \rangle$. In this case the energies associated with the states $|p\rangle$ and $|p'\rangle$ are not equal to E, and the matrix element is known as the off-shell T matrix. The differential cross section is related to the three-body T matrix which is on-shell, i.e. the energies associated with ϕ_f and ϕ_i both equal E. This is related in turn to the two-body off-shell T matrices.

Consider the three-body direct scattering process,

$$1 + (2, 3) \longrightarrow 1 + (2, 3) \qquad (1.10)$$

The three-body T operator for this process, elastic or inelastic, is T_D and this can be expressed in terms of the two-body T operators (Chen and Joachain, 1971),

$$T_D = \gamma_{21} + \gamma_{31}$$

$$\gamma_{k1} = T_k (\delta_{k2} + \delta_{k3}) + \sum_{j \neq k} T_k G_o \gamma_{j1} \qquad (1.11)$$

These are the Faddeev equations for process (1.10)
which are written more explicitly to third order
below

$$T_D = T_2 + T_3 + T_2 G_0 T_3 + T_3 G_0 T_2 + T_2 G_0 T_1 G_0 T_2$$
$$+ T_2 G_0 T_1 G_0 T_3 + T_2 G_0 T_3 G_0 T_2 + T_3 G_0 T_1 G_0 T_2$$
$$+ T_3 G_0 T_1 G_0 T_3 + T_3 G_0 T_2 G_0 T_3 + \cdots$$

$$(1.12)$$

The first order Faddeev approximation is given by
retaining only the first two terms of Equation (1.12).
These terms are purely two-body and no three-body
couplings are included in this approximation. Using
Equations (1.4), (1.6) and (1.12) we can write the
differential cross section in terms of the first
order iterate of the Faddeev equations,

$$\frac{d\sigma}{d\Omega} = \frac{\mu^2}{4\pi^2\hbar^4} \left| \langle \phi_F | T_2 + T_3 | \phi_i \rangle \right|^2 \qquad (1.13)$$

The convergence of the Faddeev expansion has been
studied rigorously (Faddeev, 1965). It has been shown
diagramatically (Chen and Joachain, 1971) that the
Faddeev expansion should have better convergence
properties than the Born series. Once the two-body
T matrices for each pair interaction are known, then
using successive iterations of the Faddeev equations
one can in principle obtain a solution of the
scattering problem.

1.4 The Coulomb problem

An extensive review of the Coulomb problem has recently
been given by Chen and Chen, (1972), and they have
shown that knowledge of the two-body off-shell Coulomb
T matrix leads in principle to a complete solution.
The properties and a particular representation of the
two-body off-shell Coulomb T matrix will be discussed
in Chapter 2. Norcliffe et.al. (1969) have obtained
correspondence identities between quantum mechanics
and classical mechanics for the two-body interaction
in momemtum space. The Faddeev equations can be used
to extend the investigation of these identities to
three body processes, where classical calculations
using Monte Carlo methods (Burgess and Percival, 1968) have
recently been made with considerable success. Using
the identities of Norcliffe et.al., we can obtain
an expression for the Coulomb T matrix which can be
expressed partially in terms of the classical
trajectories of the colliding particles. We shall
compare this expression with representations derived
by Chen and Chen (1972) and other workers.

The application of the Faddeev equations to atomic
collision processes using Chen's form of the two-body
off-shell Coulomb T matrix has been extensive in
the past five years (Chen, 1971). For low energy
problems, using a separable expansion form of the
Coulomb T matrix due to Ball et.al. (1968),
calculations of the three-body bound states for
atomic systems have been carried out successfully.

At energies above the ionization threshold the analytic form of the Coulomb T matrix is less well understood. However calculations have been carried out for many atomic scattering processes and interesting comparisons with the Born and other approximations have been obtained.

In Chapters 3 and 4, we shall use the classical path form of the Coulomb T matrix, referred to earlier, in the Faddeev equations and investigate the elastic and inelastic direct scattering of electrons on hydrogen atoms. We shall compare our results with experimental and other theoretical predictions, and conclude by assessing the use of the classical path form of the Coulomb T matrix and the Faddeev equations in predicting cross sections for atomic collision processes.

This thesis is based on a series published on the off-shell Coulomb T matrix by Roberts (1970), Hutton and Roberts (1972) and Hutton (1972).

CHAPTER 2

THE TWO-BODY COULOMB INTERACTION

2.1 Introduction

In this chapter we consider the two-body Coulomb
interaction between particles of mass m_1 and m_2
and asymptotic momenta $\underline{k}_1$ and $\underline{k}_2$. It is well
known that a complete solution of this problem
can in principle be obtained through knowledge of
the Coulomb Green function. After separating out
the total two-body momentum we can express this
function as a matrix element in relative momentum
representation, $\langle \underline{p} | G^{(+)}(E) | \underline{p}' \rangle$, where E
is the total centre of mass energy. The relative
momenta $\underline{p}$ and $\underline{p}'$, and the reduced mass in the
two-body system are given by (Chen and Chen, 1972)

$$\underline{p} = \frac{m_2 \underline{k}_1 - m_1 \underline{k}_2}{m_1 + m_2}$$

$$\mathcal{M}_{12} = \frac{m_1 m_2}{m_1 + m_2} \qquad (2.1)$$

and the two-particle kinetic energy operator is

$$H_o = \frac{p^2}{2\mathcal{M}_{12}} \qquad (2.2)$$

The two-body off-shell Coulomb T matrix is related
to the Green function by (Lippman and Schwinger, 1950),

$$\langle \underline{p} | G^{(+)}(E) | \underline{p}' \rangle = \langle \underline{p} | G_o^{(+)}(E) | \underline{p}' \rangle$$

$$+ \langle \underline{p} | G_o^{(+)}(E) | \underline{p}' \rangle \langle \underline{p} | T(E) | \underline{p}' \rangle \langle \underline{p} | G_o^{(+)}(E) | \underline{p}' \rangle \qquad (2.3)$$

Here $\langle p|G^{(+)}(E)|p'\rangle$ is the full outgoing wave Green function, and $\langle p|G_o^{(+)}(E)|p'\rangle$ is the Green function in absence of any interaction, both been given in momentum representation. Thus, having obtained an explicit form for the Coulomb Green function one should be able to deduce the scattering matrix

$\langle p|T(E)|p'\rangle$, and on substituting the latter in the Faddeev equations solve the scattering problem.

2.2 The Coulomb Green function

In momentum representation the Coulomb Green function for the relative motion of two interacting particles of charge Z_1 and Z_2 satisfies the integral equation (Perelemov and Popov, 1966),

$$\left(\frac{p^2}{2\mu_{12}}-E\right)\langle p|G(E)|p'\rangle + \frac{Z_1 Z_2 e^2}{2\pi^2\hbar}\int\frac{\langle p''|G(E)|p'\rangle}{|p-p''|^2}dp'' = -\delta(p-p') \quad (2.4)$$

Perelemov and Popov, and also Schwinger (1964) have used the symmetric transformation (Fock, 1935) to bring this equation into a form invariant with respect to the symmetry group of the hydrogen atom for negative energies, the $O(4)$ group, and for positive energies, the $O(3,1)$ group. They introduce the four vectors ξ_μ $(\mu = 0,1,2,5)$ defined as, $(i = 0,1,2,3)$,

$$\xi_i = 2p_E p_i/(p^2 + p_E^2) \cdot \qquad E < 0$$
$$\quad\quad 2p_E p_i/(p^2 - p_E^2) \qquad E > 0 \quad (2.5a)$$

$$\xi_0 = (p_E^2 - p^2)/(p_E^2 + p^2) \qquad E < 0$$
$$\quad = (p_E^2 + p^2)/(p^2 - p_E^2) \qquad E > 0 \quad (2.5b)$$

where $p_E = 2\mu_{12}|E|^{1/2}$. A point with these
coordinates lies on a four-dimensional hypersphere
which is topographically a hypersphere for $E < 0$
but for positive energies is a hyperboloid of two
sheets. The Coulomb Green function in terms of
these coordinates is,

$$G(\mathcal{E},\mathcal{E}') = \frac{-1}{16\mu_{12}p_E^3} \left(p^2 \pm p_E^2\right)^2 \langle p | G^{(+)}(E) | p' \rangle \left(p'^2 \pm p_E^2\right)^2 \quad (2.6)$$

The upper signs here (and in Equation (2.7)) refer to
the $E < 0$ case, the lower signs to the $E > 0$ case.
Equation (2.4) becomes in $\mathcal{E}$-space

$$G(\mathcal{E},\mathcal{E}') \pm \frac{\beta}{2\pi^2} \int \frac{d^3\mathcal{E}''}{\mathcal{E}_0''} \frac{G(\mathcal{E}'',\mathcal{E}')}{(\mathcal{E}-\mathcal{E}'')^2} = \delta(\mathcal{E}-\mathcal{E}') \quad (2.7)$$

where β is the Coulomb interaction parameter, $\beta = \frac{z_1 z_2 e^2 \mu_{12}}{\hbar p_E}$ (2.8).
For the $E < 0$ case Schwinger (1964) has obtained an
expression for $G(\mathcal{E},\mathcal{E}')$ in terms of the basis
functions $Y_{n\ell m}(\mathcal{E})$ of the irreducible representations
of the $O(4)$ group,

$$G(\mathcal{E},\mathcal{E}') = \sum_{n=1}^{\infty} \sum_{\ell=0}^{n-1} \sum_{m=-\ell}^{+\ell} \frac{Y_{n\ell m}(\mathcal{E}) Y_{n\ell m}^*(\mathcal{E}')}{1 + n/\beta} \quad (2.9)$$

The $Y_{n\ell m}(\mathcal{E})$ are the four-dimensional spherical
harmonics which have been studied in detail by Fock
and Bander and Itzykson (1966). They are defined on
the surface of a four-dimensional unit hypersphere
and we can define the angle χ between the vectors $\mathcal{E}$
and $\mathcal{E}'$ on the hypersphere by the relation
$|\mathcal{E}-\mathcal{E}'| = 2\sin(\chi/2)$. Making use of a summation rule
for the functions $Y_{n\ell m}(\mathcal{E})$, Perelemov and Popov were
able to formulate an expression for $G(\mathcal{E},\mathcal{E}')$ in terms
of known analytic functions,

$$G(\epsilon,\epsilon') = \delta(\epsilon-\epsilon') - \frac{\eta}{2\pi^2(\epsilon-\epsilon')^2} \tag{2.10}$$
$$+ \frac{\beta^2}{4\pi^2 i \sin\chi}\left[\Phi(e^{i\chi},\beta) - \Phi(e^{-i\chi},\beta)\right]$$

where $\Phi(z,\beta)$ is defined by

$$\Phi(z,\beta) = \sum_{n=0}^{\infty} \frac{z^n}{n+\beta} \quad , \quad |z| < 1 \tag{2.11}$$

$\Phi(z,\beta)$ can be analytically continued into the whole complex z-plane apart from the real axis cut $1 < z < \infty$.

Perlemov and Popov extended their analysis by presenting a prescription for analytic continuation of the Green function $G(\epsilon,\epsilon')$ into the whole complex plane apart from the positive real axis branch cut. For positive energies two different Green functions $G^{(\pm)}(\epsilon,\epsilon')$ are defined on the upper and lower edge of the $0 < E < \infty$ cut (Newton, p.178). In position representation these correspond to the outgoing and incoming wave Green functions, and it is the outgoing or scattered wave Green function $G^{(+)}$ which appears in Equation (2.3) for the scattering matrix. Introducing the sign function

$$\sigma = \begin{cases} +1 \text{ on the upper edge of the cut } (\epsilon = \epsilon_0 + i\delta) \\ \\ -1 \text{ on the lower edge of the cut } (\epsilon = \epsilon_0 - i\delta) \end{cases} \tag{2.12}$$

Perlemov and Popov obtain the following representation for $G(\epsilon,\epsilon')$,

$$G(\epsilon,\epsilon') = \delta(\epsilon-\epsilon') \mp \frac{\eta}{2\pi^2(\epsilon-\epsilon')^2} + \frac{\eta^2}{2\pi^2} F(\epsilon,\epsilon'') \tag{2.13}$$

where the sign $\mp$ agrees with the sign of E , and
the function $F(\epsilon, \epsilon')$ has the following integral
representations in the different regions of energy
and momentum space,

$$F(\epsilon, \epsilon') = \frac{\beta}{\sin\chi} \int_0^\infty \frac{\sinh(\pi-\chi)k}{\sinh \pi k} \frac{dk}{k^2+\beta^2} , \qquad E<0 \quad (2.14a)$$

$$F(\epsilon, \epsilon') = \frac{1}{\sinh\omega} \int_0^\infty \frac{k-\beta\coth\pi k}{k^2-\beta^2+i\sigma\delta} \sin k\omega \, dk, \qquad \begin{array}{l} E>0 \quad (2.14b) \\ p,p'>p_E \end{array}$$

$$F(\epsilon, \epsilon') = \frac{-1}{\sinh\omega} \int_0^\infty \frac{k+\beta\coth\pi k}{k^2-\beta^2+i\sigma\delta} \sin k\omega \, dk, \qquad \begin{array}{l} E>0 \quad (2.14c) \\ p,p'<p_E \end{array}$$

$$F(\epsilon, \epsilon') = \frac{\beta}{\sinh\omega} \int_0^\infty \frac{\sin k\omega}{k^2-\beta^2+i\sigma\delta} \frac{dk}{\sinh\pi k} , \qquad \begin{array}{l} E>0 \quad (2.14d) \\ p>p_E, p'<p_E \\ \text{or } p<p_E, p'>p_E \end{array}$$

For $E>0$ ω is a hyperbolic angle between the
vectors ϵ and ϵ', (which may be on different sheets
of the hyperboloid), and is defined in the different
regions of momentum space by,

$$(\epsilon-\epsilon')^2 = \begin{cases} -4\sinh^2(\omega/2) & \text{for } p,p'>p_E \text{ or } p,p'<p_E \\ \\ 4\cosh^2(\omega/2) & \text{for } p>p_E, p'<p_E \text{ or } p<p_E, p'>p_E \end{cases} \qquad (2.15)$$

Roberts (1970) has calculated the positive energy
Coulomb Green function directly in the O(3,1)
representation (Bander and Itzykson, 1966) and
transformed to momentum representation. Earlier work
by Norcliffe et.al. (1969) had shown that the spectral
operator $I_\epsilon = \lim_{\delta\to 0} (2\pi i)^{-1}(G^{(-)} - G^{(+)})$ for the Coulomb
interaction could be expressed as a sum over classical
paths, and this motivated Roberts to examine the
dependence of the Green function on classical paths.

Roberts gives the following expression for the Green
function in momentum representation,

$$\langle \underline{p} \mid G(E) \mid \underline{p}' \rangle = G_0 + G_1 + \frac{16 \mu_{12} p_E^3 \, \mathcal{G}^{(\pm)}}{\left(p^2 - p_E^2\right)^2 \left(p'^2 - p_E^2\right)^2}$$
(2.16)

where G_0 and G_1 are the well known zeroth and
first order perturbation terms. $\mathcal{G}^{(\pm)}$ has the
following different forms in $(p\text{-}p')$ - space

$$\mathcal{G}^{(\pm)} = \frac{\nu^3}{4\pi^2 \sinh\omega} \sum_{n=-\infty}^{\infty} \frac{\exp(-|n|\omega)}{n^2 + \nu^2} - \frac{\nu^2 \exp(\pm i\nu\omega)}{2\pi(1-\exp(-2\pi\nu))\sinh\omega},$$ (2.17a)
$$p, p' < p_E$$

$$\mathcal{G}^{(\pm)} = \frac{-\nu^3}{4\pi^2 \sinh\omega} \sum_{n=-\infty}^{\infty} \frac{(-1)^n \exp(-|n|\omega)}{n^2 + \nu^2} + \frac{\nu^2 \exp(-\pi\nu)\exp(\pm i\nu\omega)}{2\pi(1-\exp(-2\pi\nu))\sinh\omega}$$ (2.17b)

$$p > p_E , \; p' < p_E \quad \text{or} \quad p < p_E , \; p' > p_E$$

$$\mathcal{G}^{(\pm)} = \frac{\nu^3}{4\pi^2 \sinh\omega} \sum_{n=-\infty}^{\infty} \frac{\exp(-|n|\omega)}{n^2 + \nu^2} - \frac{\nu^2 \exp(-2\pi\nu)\exp(\pm i\nu\omega)}{2\pi(1-\exp(-2\pi\nu))\sinh\omega}$$ (2.17c)

$$p, p' < p_E$$

where the hyperbolic angle is defined by

$$1 + \frac{2p_E^2 |\underline{p}-\underline{p}'|^2}{(p^2-p_E^2)(p'^2-p_E^2)} = \begin{array}{l} +\cosh\omega, \quad p,p' > p_E \text{ and } p,p' < p_E \\ \\ -\cosh\omega, \quad p > p_E , p' < p_E \text{ and } p < p_E , p' > p_E \end{array}$$
(2.18)

and ν is defined slightly differently from the $\mathfrak{z}$
of Perelemov and Popov by

$$\nu = \frac{|z_1 z_2| e^2 \mu_{12}}{\hbar p_E} .$$
(2.19)

Before examining the significance of the different
terms in this expression, we shall demonstrate the
equivalence of the forms of the Coulomb Green function

given by Perelemov and Popov and by Roberts.

The discussion is limited to the attractive Coulomb scattering of two particles of unit charge. We shall evaluate the scattered wave Green function $G^{(+)}$ in the region of momentum space $p \cdot p' > p_E$, which for attractive scattering is the classically accessible region (Norcliffe et.al., 1969). Calculations of $G^{(+)}$ for the other regions of momentum space are similar, and can be inferred from the results of this calculation.

One can use the summation rule for the four-dimensional spherical harmonics to express the second term in Equation (2.13) in integral form. One obtains the expression(Perelemov and Popov, 1966).

$$\frac{1}{2\pi^2 (\epsilon - \epsilon')^2} = \frac{-1}{4\pi^2 \sinh w} \int_0^\infty d\rho \, \coth(\pi\rho/2) \sin(\rho w/2) \quad (2.20)$$

Substituting this equality back into equation (2.13) and using equation (2.6) we obtain the Coulomb Green function in momentum representation,

$$G(p, p'; E) = \frac{-16 \mu_{12} \, p_E^3 \, \delta(\epsilon - \epsilon')}{(p^2 - p_E^2)^2 (p'^2 - p_E^2)^2}$$

$$\frac{-16 \mu_{12} \, p_E^3 \, \beta}{4\pi^2 \sinh w \, (p^2 - p_E^2)^2} \left[-\frac{1}{2} \int_{-\infty}^\infty d\rho \, \coth(\pi\rho/2) \sin(\rho w/2) \right.$$

$$\left. + \beta \int_{-\infty}^\infty dk \, \frac{k - \beta \coth \pi k}{k^2 - \beta^2 + i\delta} \sin k w \right] \frac{1}{(p'^2 - p_E^2)^2} \qquad (2.21)$$

The first term in this expression is equivalent to the G_0 of Equation (2.16). The remaining integrals can be evaluated quite simply using contour integral methods and the residue theorem.

Consider the first term in the square brackets of Equation (2.21). The integrand has an infinite set of poles at $\sinh(\pi \rho/2) = 0$. We shall use the residue theorem to integrate the function $F(z) = \coth(\pi z/2) \exp(i z \omega/2)$ around the contour C which is shown in Figure (2.1) along with a schematic representation of the poles of $F(z)$ lying within C. The poles of $F(z)$ are at $z = 2ni$ where n is an integer $0 \leq n < \infty$ and each pole contributes a residue $(2/\pi) \exp(-n\omega)$ to the integral. In the limit $R \to \infty$ the integral along the arc Γ approaches zero (Spiegel, p.172), and the infinite set of poles contribute to the result

$$\int_{-\infty}^{\infty} d\rho \; \sin(\rho\omega/2) \coth(\pi\rho/2) = 4 \sum_{n=0}^{\infty} \exp(-n\omega) \quad (2.22)$$

The integrand $k \sin k\omega / (k^2 - \beta^2 + i\delta)$ has two simple poles at $k = \pm(\beta - i\delta/2\beta)$. The function $g(z) = z \exp(i z \omega)/(z^2 - \beta^2 + i\delta)$ has only one pole inside the contour C_1 of Figure (2.2) at $z = -\beta + i\delta/2\beta$, and using the residue theorem and taking the limit $\delta \to 0$ (a specification of the analytic continuation for the Coulomb Green function) we obtain the result,

FIGURE 2.1: THE CONTOUR C
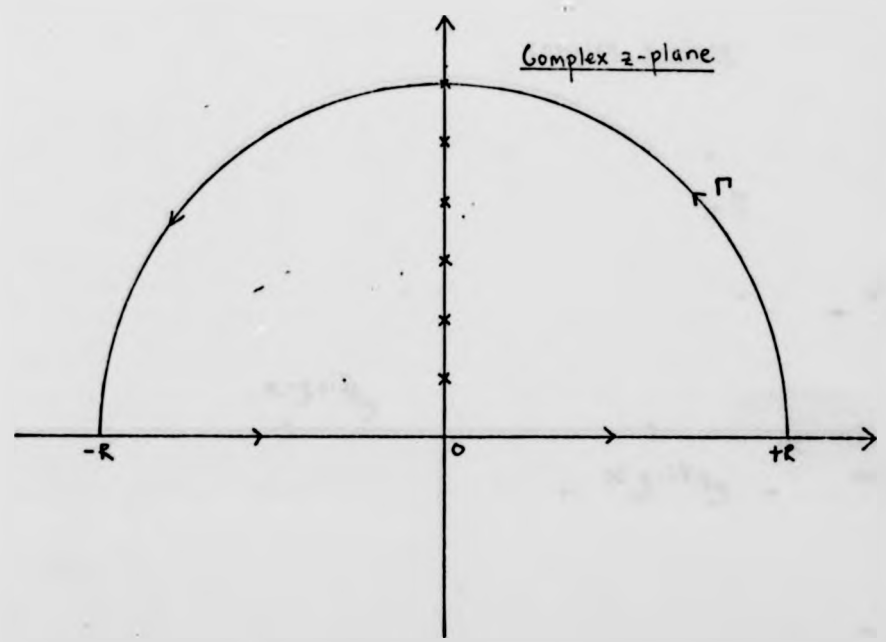
x indicates poles of $F(z) = \coth\left(\frac{\pi z}{2}\right) \exp\left(iz\frac{w}{2}\right)$ lying within Contour C.

FIGURE 2.2. THE CONTOUR C_1

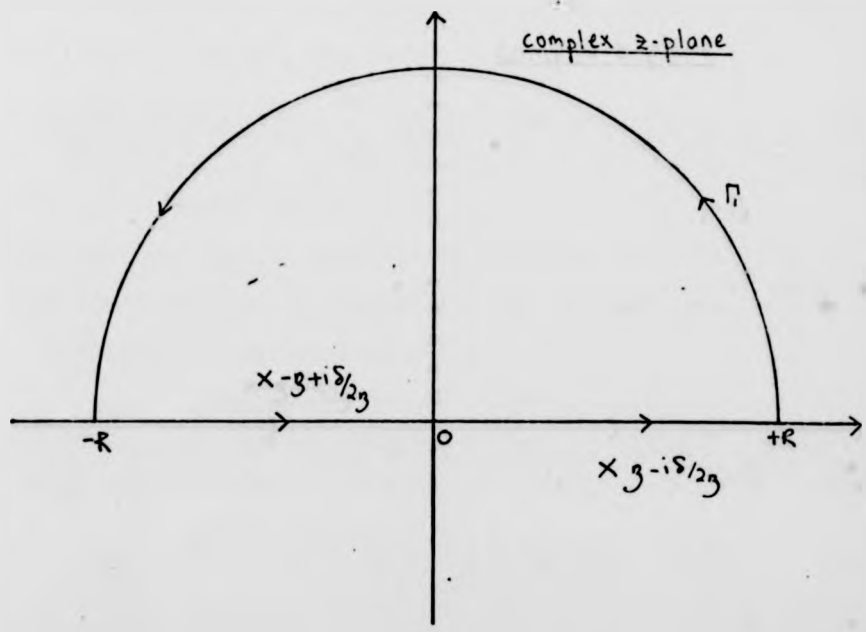x indicates poles of $g(z) = z \exp(izw)/(z^2 - g^2 + i\delta)$. Only one pole lies within C_1.

FIGURE 23: THE CONTOUR C_3
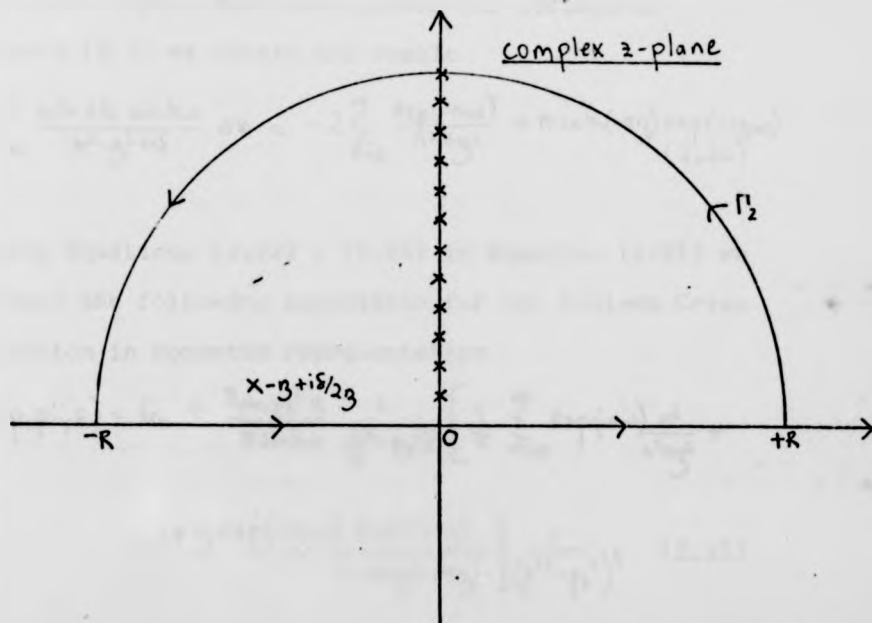
x indicates poles of $h(z) = \coth(\pi z)\exp(izw)/(z^2 - g^2 + i\delta)$ lying within C_2

$$\int_{-\infty}^{\infty} \frac{k \sin k\omega}{k^2 - g^2 + i\delta} \, dk = \pi \exp(-ig\omega) \qquad (2.23)$$

Finally the integrand $\coth(\pi k)\sin k\omega / (k^2 - g^2 + i\delta)$ has an infinite set of poles at $k = ni$, and two simple poles at $k = \pm(g - i\delta/2g)$. Integrating the function $h(z)$ around the contour C_2 defined in Figure (2.3) we obtain the result

$$\int_{-\infty}^{\infty} \frac{\coth \pi k \sin k\omega}{k^2 - g^2 + i\delta} \, dk = -2 \sum_{n=0}^{\infty} \frac{\exp(-n\omega)}{n^2 + g^2} + \pi \coth(-\pi g) \exp(-ig\omega) \qquad (2.24)$$

Using Equations (2.22) - (2.24) in Equation (2.21) we obtain the following expression for the Coulomb Green function in momentum representation

$$G(\rho, \rho'; E) = G_0 + \frac{8\mu_{12} p_E^3 g}{\pi \sinh \omega} \frac{1}{(p^2 - p_E^2)^2} \left[\frac{1}{\pi} \sum_{n=0}^{\infty} \exp(-n\omega) \frac{n^2}{n^2 + g^2} + \right.$$

$$\left. + g \exp(-ig\omega) \frac{\exp(-2\pi g)}{1 - \exp(-2\pi g)} \right] \frac{1}{(p'^2 - p_E^2)^2} \qquad (2.25)$$

Using the equality

$$\sum_{n=0}^{\infty} \exp(-n\omega) \frac{n^2}{n^2 + g^2} = \sum_{n=0}^{\infty} \exp(-n\omega) - g^2 \sum_{n=0}^{\infty} \frac{\exp(-n\omega)}{n^2 + g^2} \qquad (2.26)$$

and the transformations between E-space and ρ-space given by Perelemov and Popov, we can write for the first term in the square brackets,

$$\frac{g}{2\pi^2 \sinh \omega} \sum_{n=0}^{\infty} \exp(-n\omega) \frac{n^2}{n^2 + g^2} = \frac{g}{8\pi^2 p_E} \frac{(p^2 - p_E^2)(p'^2 - p_E^2)}{|p - p'|^2} -$$

$$- \frac{g^3}{4\pi^2 \sinh \omega} \sum_{n=-\infty}^{\infty} \frac{\exp(-|n|\omega)}{n^2 + g^2} \qquad (2.27)$$

Hence the Coulomb Green function is given by

$$\langle \rho |G(\varepsilon)| \rho' \rangle = G_0 + \frac{16 \mu_{12} \rho_\varepsilon^3}{(\rho^2 - \rho_\varepsilon^2)^2 (\rho'^2 - \rho_\varepsilon^2)^2} \left[\frac{3}{8\pi^2 \rho_\varepsilon^2} \frac{(\rho^2 - \rho_\varepsilon^2)(\rho'^2 - \rho_\varepsilon^2)}{|\rho - \rho'|^2} - \right.$$

$$\left. - \frac{3^3}{4\pi^2 \sinh w} \sum_{n=-\infty}^{\infty} \frac{\exp(-|n|w)}{n^2 + 3^2} + \frac{3^2}{2\pi \sinh w} \frac{\exp(-i 3 w)\exp(-2\pi 3)}{1 - \exp(-2\pi 3)} \right] \quad 28)$$

This is similar in form to the expressions (2.16) and (2.17a) of Roberts, the differences being due to the different definitions of 3 and ϑ for attractive scattering. Perelemov and Popov define 3 to be **negative** for attractive **scattering (Equation (2.8))**, **wheras ϑ is positive for both the repulsive and the** attractive case (Equation (2.19)), and noting that the first term in the square brackets of (2.28) is just G_1 of (2.16), we see that Perelemov and Popov's form of the Coulomb Green function for $\varepsilon > 0$ and $\rho, \rho' > \rho_\varepsilon$ is exactly the same as the form (2.16) derived by Roberts, **if we redefine 3 as $-\vartheta$.**

We note that the transformation $3 \to -\vartheta$ could be carried out at the beginning of the analysis in (2.13) and (2.14b). In this case care must be exercised in the analytic continuation, and the sign of δ in the denominator of the integrand of Equation (2.14b) is changed. Then the results (2.16) and (2.17a) of Roberts are directly obtained after an analysis similar to the one we have performed.

Using Equations (2.14c) and (2.14d) and the same
method of analysis one can obtain the equivalent
results (2.17b) and (2.17c) of Roberts for the
other regions of momentum space.

Therefore the method of Perelemov and Popov in which
the Coulomb Green function is evaluated for $E < 0$
and analytically continued to give $G^{(\pm)}$ for $E > 0$
is shown to be equivalent to the method of Roberts
in which $G^{(\pm)}$ is calculated directly for $E > 0$.
Chen and Chen (1972) have demonstrated the equivalence
of the form of $G^{(\pm)}$ derived by Perelemov and Popov
with the forms derived by Schwinger (1964), Hostler
(1964) and Okubo and Feldman (1960) which implies
that the Roberts expression is equivalent to all of
these forms. The Roberts form of $G^{(\pm)}$ is such that
it can be partially expressed as a sum over classical
paths, and it is this form which we will concern
ourselves with in this thesis.

The Coulomb Green function is analytic everywhere in
the complex energy plane apart from the physical
energy spectrum. It is singular at the bound state
energy levels for $E < 0$, and along the continuum
cut representing the energy continuum for $E > 0$.
These properties have important consequences for the
two-body off-shell Coulomb T matrix and will be
considered in more detail in the following sections.

2.3 The Spectral Operator

A correspondence identity for the spectral operator, $\delta(E-H)$, for positive energy Coulomb scattering has been demonstrated by Norcliffe et.al. (1969). The diagonal elements of the kernel of the spectral operator in momentum representation are proportional to the quantal microcanonical momentum distribution $\rho_E^{qm}(\underline{p})$. Evaluating this quantity from our results for $G^{(\pm)}$ in the classical limit and comparing it with the classical microcanonical momentum distribution $\rho_E^{cm}(\underline{p})$ provides a useful check on our results.

From (2.16) and (2.17a) - (2.17c) we have for the spectral operator

$$\langle \underline{p} | \delta(E-H) | \underline{p}' \rangle = \frac{1}{2\pi i} \langle \underline{p} | (G^{(-)} - G^{(+)}) | \underline{p}' \rangle$$

$$= \frac{8 \mu_{12}^3 \, p_E \, k^2 \, g(\nu)}{\pi^2 \hbar^2 (p^2 - p_E^2)^2 (p'^2 - p_E^2)^2 (1 - \exp(-2\pi\nu))} \frac{\sin \nu \omega}{\sinh \omega} \quad (2.29)$$

where k is given by $k = Z_1 Z_2 \, e^2$

and

$$g(\nu) = \begin{array}{l} 1 \quad \text{for} \quad p, p' > p_E \\ -\exp(-\pi\nu) \quad \text{for} \quad p > p_E, p' < p_E \text{ or } p < p_E, p' > p_E \\ \exp(-2\pi\nu) \quad \text{for} \quad p, p' < p_E \end{array} \quad (2.30)$$

Banks (Norcliffe et.al., 1969) has calculated $\rho_E^{cm}(\underline{p})$ normalised to unit inward flux, and for attractive scattering the result is

$$\rho_E^{CM}(p) = \frac{64 \pi k^3 \mu_{12}^4}{p_E^2 (p^2 - p_E^2)^4} \times \begin{array}{l} 1 \text{ for } p > p_E \\ 0 \text{ for } p < p_E \end{array} \quad (2.31)$$

Taking the limit $p \to p'$ of Equation (2.29) and using the same normalisation as in the classical evaluation, Norcliffe et.al. obtained the following expression for $\rho_E^{qm}(p)$,

$$\rho_E^{qm}(p) = \frac{64 \pi k^3 \mu_{12}^4}{p_E^2 (p^2 - p_E^2)^4 (1 - \exp(-2\pi\nu))} \times \begin{array}{l} 1 \text{ for } p > p_E \\ \exp(-2\pi\nu) \text{ for } p < p_E \end{array} \quad (2.32)$$

From Equation (2.19) we see that ν is proportional to $\hbar^{-1}$ and in the classical limit when $\hbar \to 0$ then ν becomes infinite. Equivalently we could say that ν is infinite for large principle quantum number, n . In this limit Equation (2.32) reduces to Equation (2.31). Thus the classical limit of $\rho_E^{qm}(p)$ derived from our results agrees exactly with the classical result.

Dividing the momentum space as shown in Figure (2.4), then the region III, where $p, p' < p_E$, is classically inaccessible for attractive Coulomb scattering, and this is confirmed by the fact that $\rho_E^{CM}(p) = 0$ in this region. Quantum mechanically, barrier penetration into region III is a possibility, this fact being indicated by the non-zero momentum distribution for the $p < p_E$ region in (2.32). However on taking the

FIGURE 2.4
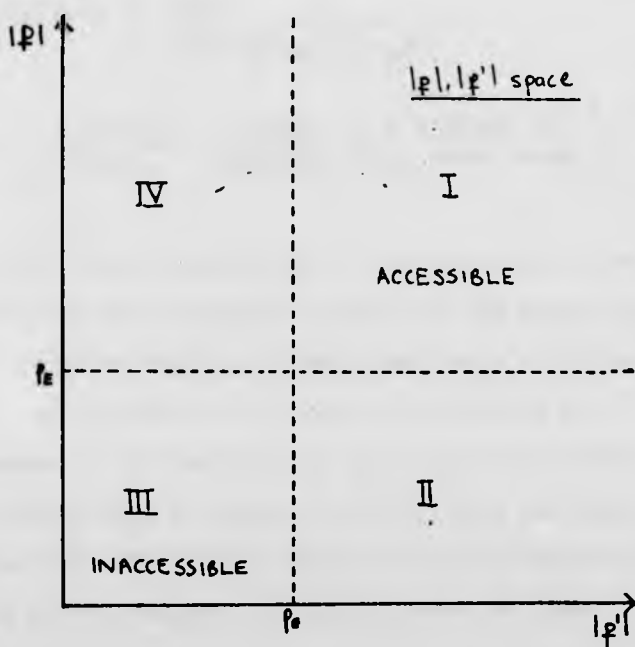
The classical picture of momentum space
for attractive scattering.

classical limit of (2.32), the effects of barrier
penetration are seen to disappear and the classical
result (2.31) is obtained.

2.4 The Coulomb T matrix

Substituting the expression for the scattered wave
Coulomb Green function (2.25) into Equation (2.3), we
obtain the form for the T matrix

$$\langle \rho | T(E) | \rho' \rangle = \frac{4 \rho_E^3 \gamma}{2 \pi \mu_\Omega} \frac{1}{(\rho^2 - \rho_E^2)(\rho'^2 - \rho_E^2)} \times$$

$$\times \left[\frac{\gamma \exp(-i\gamma w)}{\sinh w} \frac{\exp(-2\pi\gamma)}{1 - \exp(-2\pi\gamma)} + \frac{1}{\pi} \sum_{n=0}^{\infty} \frac{\exp(-nw)}{\sinh w} \frac{n^2}{n^2 + \gamma^2} \right] \quad (2.33)$$

This is exactly equivalent to the expression derived
by Shastry and Rajagopal (1972) for the region $\rho, \rho' > \rho_E$.
For the other regions of momentum space a similar
analysis reproduces the results of Shastry and
Rajagopal. The analysis of Chen and Chen (1972) implies
the equivalence of Equation (2.33), and its extension
to the rest of momentum space, with the various other
forms of the Coulomb T matrix cited by Chen.

An alternative form is obtained by substituting the
Roberts form of the scattered wave Coulomb Green
function (2.16) and (2.17a-c) in Equation (2.3).
Then the Coulomb T matrix can be expressed as a
sum of three terms (Roberts, 1971)

$$\langle \rho | T(E) | \rho' \rangle = T_b + T_p + T_c \quad (2.34)$$

where

$$T_B = \frac{-P_c}{2\pi^2 \mu_{12} |p-p'|^2} \tag{2.35a}$$

$$T_P = \frac{P_c^3}{4\pi^2 \mu_{12}^3 |E-T||E-T'| \sinh\omega} \sum_{n=-\infty}^{\infty} \frac{\xi^n \exp(-|n|\omega)}{n^2 + \nu^2} \tag{2.35b}$$

$$T_C = \frac{-P_c^3 \, g(T,T') \exp(i\nu\omega)}{2\pi \nu \mu_{12}^3 |E-T||E-T'|(1-\exp(-2\pi\nu)) \sinh\omega} \tag{2.35c}$$

where $P_c = |z_1 z_2| e^2 \mu_{12}/\hbar$, $T = P^2/2\mu_{12}$, $T' = P'^2/2\mu_{12}$

and

$$g(T,T') = \begin{array}{ll} 1 & \text{for } T,T' > E \\ \exp(-\pi\nu) & \text{for } T > E, T' < E \text{ or } T < E, T' > E \\ \exp(-2\pi\nu) & \text{for } T, T' < E \end{array} \tag{2.36}$$

$$\xi = \text{sign} (E-T)(E-T')$$

T_B is just the first Born approximation to the T matrix given by Equation (1.5). T_P, which we call the pole term, is related to the bound state poles of the Coulomb Green function. At negative energies singularities appear in T_P for $n = \pm\nu$ which correspond to the bound state energy levels of the hydrogen atom. The third term, T_C, contains a factor $g(T,T')[1-\exp(-2\pi\nu)]^{-1}\exp(i\nu\omega)$ which Norcliffe et.al. (1969) have shown can be expressed as a sum over classical paths. T_C is thus called the classical path term.

The classical paths are defined in the normal sense only in the classically accessible region I of

Figure (2.4). In this region the path connecting
the momenta p and p' contributes to T_c an
amount proportional to the cosine (sine) of the
classical action in units of $\hbar$ along the path.
Norcliffe et.al. (1969) show that

$$\frac{-\nu^2}{2\pi \sinh \omega} \frac{\exp(i\nu\omega)}{1 - \exp(-2\pi\nu)} = \nu^2 \sum_{c=0}^{\infty} \frac{\exp\left[i S_c(p, p'; \varepsilon)/\hbar\right]}{2\pi \sin(\text{analytic path length})} \quad (2.37)$$

where S_c is the classical action for c complete
orbits from p to p' . For the case where the path is
directly along the arc from p to p' the action is

$$S_0 \equiv \int_{p'}^{p} \underline{r} \cdot d\underline{p}'' \quad (2.38)$$

In analogy with barrier penetration in the quantum
mechanical case, classical paths may exist in the
classically inaccessible region III, but not in the
normal sense. The paths are the analytic continuations
of the classically allowed paths and an infinite number
of these paths may connect any two points p and p'
within or without the classically accessible region.

The real significance of Equation (2.34) lies in its
on-shell limit when $T, T' \to E$. The scattering
amplitude $f(E, \theta)$ for scattering at an energy E through
an angle θ for short range potentials is proportional
to the on-shell limit of the T matrix. Hence taking
the on-shell limit of each term in Equation (2.32) will

give us an expression which can be compared with the
scattering amplitude. It is found (Roberts, 1971)
that the on-shell limits of T_B and T_P are equal and
opposite. Thus the scattering amplitude is to be
compared with the on-shell limit of a term which may
be expressed as a sum over classical paths.

Ford (1964) and Schwinger (1964) have demonstrated
that the on-shell limit of the Coulomb T matrix does
not exist in a strictly mathematical sense due to the
long range nature of the Coulomb potential. However,
Schwinger (1964) has shown that if the free wave Green
function in Equation (2.3) is replaced near the energy
shell by the distorted wave Green function, $\tilde{G}_0^{(+)}$,
which accounts for the Coulomb distortion, then the
Rutherford scattering amplitude is obtained from the
on-shell limit of T_C. This on-shell correspondence
identity leads to the possibility that cross sections
in atomic scattering processes can be expressed
in terms of a sum over classical paths.

2.5 The $E<0$ Coulomb T matrix

The T matrix we have dealt with so far is the positive
energy T matrix. Contributions from the $E<0$ Coulomb
T matrix are not of much concern to us in
scattering calculations, however in certain cases they
are relevant. We therefore quote the results obtained
by Roberts (private communication) for the $E<0$ T
matrix which can be evaluated directly from the

give us an expression which can be compared with the scattering amplitude. It is found (Roberts, 1971) that the on-shell limits of T_B and T_P are equal and opposite. Thus the scattering amplitude is to be compared with the on-shell limit of a term which may be expressed as a sum over classical paths.

Ford (1964) and Schwinger (1964) have demonstrated that the on-shell limit of the Coulomb T matrix does not exist in a strictly mathematical sense due to the long range nature of the Coulomb potential. However, Schwinger (1964) has shown that if the free wave Green function in Equation (2.3) is replaced near the energy shell by the distorted wave Green function, $\tilde{G}_o^{(+)}$, which accounts for the Coulomb distortion, then the Rutherford scattering amplitude is obtained from the on-shell limit of T_C. This on-shell correspondence identity leads to the possibility that cross sections in atomic scattering processes can be expressed in terms of a sum over classical paths.

2.5 The $E<0$ Coulomb T matrix

The T matrix we have dealt with so far is the positive energy T matrix. Contributions from the $E<0$ Coulomb T matrix are not of much concern to us in scattering calculations, however in certain cases they are relevant. We therefore quote the results obtained by Roberts (private communication) for the $E<0$ T matrix which can be evaluated directly from the

$E < 0$ Coulomb Green function representation of Perelemov and Popov. For attractive scattering we have

$$\langle p|T(E)|p'\rangle = \frac{p_c^3}{2\pi^2 \mu_{12}{}^3 (E-T)(E-T')\sin\chi} \times$$

$$\times \left[\int_0^\infty \frac{\sinh(\pi-\chi)k\ dk}{(k^2+\nu^2)\sinh\pi k} - \frac{i\pi\sin\nu\chi}{\nu} \sum_{c=-\infty}^\infty \cos 2n\chi \right] (2.39)$$

where χ is defined in Section (2.2). The second term, which is omitted in the Perelemov and Popov representation, is due to the fact that for attractive scattering when $\nu = -\zeta$ is positive the $\Phi(z,\nu)$ of Equation (2.11) can be singular. Perelemov and Popov have just considered the principle part of this function and have omitted the δ-function which is associated with the singularity.

For repulsive scattering $\Phi(z,\nu)$ has no singularities and we obtain straight forwardly for the repulsive scattering $E < 0$ Coulomb T matrix

$$\langle p|T(E)|p'\rangle = \frac{-p^3}{2\pi^2\mu_{12}{}^3(E-T)(E-T')\sin\chi} \int_0^\infty \frac{\sinh(\pi-\chi)k\ dk}{(k^2+\nu^2)\sinh\pi k} \quad (2.40)$$

2.6 Properties of the two-body off-shell Coulomb T matrix

A comprehensive account of the properties of the Coulomb T matrix has been given in the review of Chen and Chen (1972), so here we will just briefly mention the properties which concern us most.

The Coulomb T matrix, like the Green function, is analytic everywhere in the complex energy plane apart from the bound state poles and the continuum cut. It is defined on either side of the continuum cut and several authors (Chen and Chen, 1972, Nuttall and Stagat, 1971) have demonstrated that it satisfies a modified unitarity relation. Indeed Roberts (1971) has demonstrated that the unitarity relation is related to the spectral operator and thus to classical paths by (note error in Roberts' result)

$$\langle \rho |(T-T^{+})|\rho' \rangle = -(2\pi i)(E-T)(E-T')\langle \rho|\delta(E-H)|\rho'\rangle \quad (2.41)$$

We have **already** mentioned that the Coulomb T matrix has singularities on the energy shell. It also has singularities on the half-energy shell, that is when $T \to E$ or $T' \to E$. These singularities lead to the factors $g(T,T')$ in the expression for T_c. In practical applications great care must be taken with these factors on integrating the T matrix over the momentum variables.

2.7 Summary

To conclude this chapter we summarise the results for the form of the two-body off-shell Coulomb T matrix which we shall utilise in the Faddeev equations to solve several atomic collision problems in the next two chapters.

i) Attractive scattering

$$\langle p|T(E)|p'\rangle = T_B + T_P + T_C$$

$$T_B = \frac{-\rho_c}{2\pi^2\mu_{12}|p-p'|^2}$$

$$T_P = \frac{\rho_c^3}{4\pi^2\mu_{12}^3|E-T||E-T'|\sinh w}\sum_{n=-\infty}^{\infty}\frac{\xi^n\exp(-|n|w)}{n^2+\nu^2}$$

$$T_C = \frac{-\rho_c^3}{2\pi\nu\mu_{12}^3|E-T||E-T'|\sinh w}\frac{\mathcal{g}(T,T')\exp(i\nu w)}{1-\exp(-2\pi\nu)}$$

$$\xi = \text{sign}(E-T)(E-T')$$

$$\mathcal{g}(T,T') = \begin{array}{ll} 1 & \text{for } T,T'>E \\ \exp(-\pi\nu) & \text{for } T>E, T'<E \text{ and } T<E, T'>E \\ \exp(-2\pi\nu) & \text{for } T,T'<E \end{array}$$

$$\nu = \rho_c/\rho_E \qquad , \quad \rho_c = |z_1 z_2|e^2\mu_{12}/\hbar$$

$$1 + \frac{2\rho_E^2|p-p'|^2}{(p^2-\rho_E^2)(p'^2-\rho_E^2)} = \begin{array}{ll} +\cosh w & \text{for } T,T'>E \text{ and } T,T'<E \\ -\cosh w & \text{for } T>E, T'<E \text{ and } T<E, T'>E. \end{array}$$

ii) Repulsive scattering

For the case of repulsive scattering we must change
the sign of the Coulomb interaction factor ρ_c .
The results then become

$$\langle p|T(E)|p'\rangle = .T_B + T_P + T_C$$

$$T_B = \frac{\rho_c}{2\pi^2\mu_{12}|p-p'|^2} \qquad\qquad (2.42a)$$

$$T_P = \frac{-p_c^3}{4\pi^2 \mu_{12}^3 |E-T||E-T'| \sinh\omega} \sum_{n=-\infty}^{\infty} \frac{\xi^n \exp(-|n|\omega)}{n^2+\nu^2} \quad (2.42b)$$

$$T_C = \frac{p_c^3 \, g(T,T') \exp(-i\nu\omega)}{2\pi \mu_{12}^3 |E-T||E-T'|(1-\exp(-2\pi\nu))\sinh\omega} \quad (2.42c)$$

$$\xi = \text{sign}(E-T)(E-T')$$

$$g(T,T') = \begin{cases} \exp(-2\pi\nu) & \text{for } T,T' > E \\ \exp(-\pi\nu) & \text{for } T>E, T'<E \text{ and } T<E, T'>E \\ 1 & \text{for } T,T' < E \end{cases}$$

$$\nu = p_c/p_E \quad, \quad p_c = -|z_1 z_2| e^2 \mu_{12}/\hbar$$

and ω is defined the same as in the attractive case.
For repulsive scattering the classically accessible
region is region III where $\quad p, p' < p_E \quad$.

CHAPTER 3

THE ELASTIC e-H SCATTERING PROBLEM

3.1 Introduction

One of the most fundamental three-body processes in
atomic collision physics is the elastic scattering of
electrons by atomic hydrogen in its ground state.
This direct collision process is represented by

$$1 + (2,3) \longrightarrow 1 + (2,3) \tag{3.1}$$

where 1 is the incident electron, and we designate 2
to be the bound electron and 3 to be the proton.

The transition amplitude for the process (3.1) is the
matrix element $\langle f | T_D | i \rangle$ where $|i\rangle$ and $|f\rangle$
represent respectively the initial and final 'free' states
of the system. In the first order iterate of the Faddeev
equations the three-body T operator, T_D , is the sum
of two terms, T_2 and T_3 . T_2 is the two-body off-shell
Coulomb T operator in the three-particle Hilbert space
for the interaction between the incident electron and the
proton, with the bound electron as a spectator particle,
and similarly T_3 represents the incident electron
interaction with the bound electron. The expressions for
the two-body off-shell Coulomb T matrix (Equations (2.34) -
(2.36), (2.42)) will be utilised to calculate the
transition amplitude.

The scattering amplitude, $F(E,\theta)$, for the e-H scattering process is given in terms of the transition amplitude by (Newton, p.219)

$$F(E,\theta) = -4\pi^2 \mu_1 \langle F|T_D|i\rangle \qquad (3.2)$$

where μ_1 is the mass of particle 1, the incident electron, reduced relative to the centre of mass of the $(2,3)$ particle system. The scattering amplitude is complex and the differential cross section, $d\sigma/d\Omega$, is given by

$$\frac{d\sigma}{d\Omega} = |F(E,\theta)|^2 \qquad (3.3)$$

The asymptotic momentum of the incident electron is q_i initially and q_f finally. The energy conservation relation for the system is

$$E_i + q_i^2/2\mu_1 = E_F + q_f^2/2\mu_1 \qquad (3.4)$$

where E_i and E_F are respectively the initial and final bound state energies of the hydrogen atom. For the case of elastic scattering from the ground state $|q_i| = |q_f|$, and $E_i = E_F = E_{1S} = -\beta^2/2\mu_{23}$, where β is the Bohr momentum for the ground state of hydrogen and μ_{23} is the reduced mass of the $(2,3)$ two-particle system.

The Faddeev equations and the derived forms of the two-body off-shell Coulomb T matrix are in the momentum representation. It is therefore convenient to work in the barycentric coordinate system which is described in the next section.

3.2   The Barycentric Coordinate System

The collision process is shown schematically in Figure (3.1). The transition amplitude is $\langle F | T_b | i \rangle$

$$\underset{e_1^-}{\bullet \!\longrightarrow}$$

$$\text{FIGURE } 3.1$$

and the initial and final 'free' states are given in the barycentric coordinates appropriate to the initial conditions by

$$\langle \underline{P}\, q_2\, q_{23} | i \rangle = \delta(\underline{P}-\underline{P}_i)\, \delta(q_2-q_i)\, \phi_{1s}(q_{23}) \qquad (3.5a)$$

$$\langle \underline{P}\, q_2\, q_{23} | F \rangle = \delta(\underline{P}-\underline{P}_F)\, \delta(q_2-q_F)\, \phi_{1s}(q_{23}) \qquad (3.5b)$$

The barycentric coordinate relations to the laboratory coordinates are shown in Figure (3.2). The total momentum vector of the system is $\underline{P}$, the subscript i and F indicating respectively its initial and final values. The coordinate q_2 is the momentum of e_1^- relative to the centre mass of the $(2,3)$ system, and

q_{23} is the relative momentum of e_2^- and p_3^+ in their own centre of mass frame. The coordinates q_2 and q_{23} are conjugate momenta and a cyclic permutation of the subscripts is allowed depending on the initial conditions (Chen et.al., 1969), so that the states $|i\rangle$ and $|F\rangle$ could equally be defined on the $|\underline{P}\, q_2\, q_{31}\rangle$ basis or the $|\underline{P}\, q_3\, q_{12}\rangle$ basis. The $\delta(q_2-q_i)$ factor in Equation (3.5a)

FIGURE 3.2: THREE-BODY COORDINATE SYSTEM AND KINEMATICS

LABORATORY

Charge	Mass	Position	Momentum
z_1e	m_1	r_1	$p_1 = m_1 \dfrac{dr_1}{dt}$
z_2e	m_2	r_2	$p_2 = m_2 \dfrac{dr_2}{dt}$
z_3e	m_3	r_3	$p_3 = m_3 \dfrac{dr_3}{dt}$

Kinetic Energy
$$T = \frac{p_1^2}{2m_1} + \frac{p_2^2}{2m_2} + \frac{p_3^2}{2m_3}$$

Potential Energy
$$\langle r_1 r_2 r_3 | V_{23} | r_1' r_2' r_3' \rangle = \delta(r_1 - r_1')\,\delta(r_2 - r_2')\,\delta(r_3 - r_3')\,\frac{z_2 z_3 e^2}{|r_2 - r_3|}$$

BARYCENTRIC (+cyclic permutations)

Charge	Mass	Position	Momentum
z_1e	$M = m_1 + m_2 + m_3$	$R = \dfrac{m_1 r_1 + m_2 r_2 + m_3 r_3}{m_1 + m_2 + m_3}$	$P = p_1 + p_2 + p_3 = M\dfrac{dR}{dt}$
z_1e	$M_1 = \dfrac{m_1(m_2 + m_3)}{M_1 + m_2 + m_3}$	$\rho_1 = r_1 - \left(\dfrac{m_2 r_2 + m_3 r_3}{m_2 + m_3}\right)$	$q_1 = \dfrac{(m_2 + m_3)p_1 - m_1(p_2 + p_3)}{m_1 + m_2 + m_3} = M_1 \dfrac{d\rho_1}{dt}$
z_3e	$M_{23} = \dfrac{m_2 m_3}{m_2 + m_3}$	$\rho_{23} = r_2 - r_3$	$q_{23} = \dfrac{m_3 p_2 - m_2 p_3}{m_2 + m_3} = M_{23}\dfrac{d\rho_{23}}{dt}$

Kinetic Energy
$$T = \frac{P^2}{2M} + \frac{q_1^2}{2M_1} + \frac{q_{23}^2}{2M_{23}} = \text{(cyclic permutations)}$$

Potential Energy
$$\langle R \rho_1 \rho_{23} | V_{23} | R' \rho_1' \rho_{23}' \rangle = \delta(R - R')\,\delta(\rho_1 - \rho_1')\,\delta(\rho_{23} - \rho_{23}')\,\frac{z_2 z_3 e^2}{\rho_{23}}$$

$$\langle \rho_1 q_{23} | V_{23} | \rho_1' q_{23}' \rangle = \delta(\rho_1 - \rho_1')\,\delta(q_1 - q_1')\,\left(z_2 z_3 e^2 / 2\pi^2 \hbar\, |q_{23} - q_{23}'|^2\right)$$
$$= \delta(\rho_1 - \rho_1')\,\delta(q_1 - q_1')\,\langle q_{23} | \hat{V}_{23} | q_{23}' \rangle .$$

represents an initial plane wave state for the incident electron in the momentum representation, while $\phi_{1s}(q_i)$ is the ground state wave function of the hydrogen atom in momentum space. The total energy, E , of the system is

$$E = \frac{P_i^2}{2M} + \frac{q_i^2}{2\mu_1} + E_{1s} \qquad (3.6)$$

where M and μ_1 are defined in Figure (3.2).

The matrix elements $\langle F|T_2|i\rangle$ representing the electron-proton contribution to the scattering amplitude and $\langle F|T_3|i\rangle$ representing the electron-electron contribution are evaluated separately. The momentum representation of T_2 using the appropriate barycentric coordinates is

$$\langle \underline{P}\ q_2\ q_{31}|T_2(E)|\underline{P}'\ q_2'\ q_{31}'\rangle$$
$$= \delta(\underline{P}-\underline{P}')\ \delta(q_2-q_2')\langle q_{31}|T_2\left(E-\frac{P^2}{2M}-\frac{q_2^2}{2\mu_2}\right)|q_{31}'\rangle \quad (3.7)$$

Physically $\delta(\underline{P}-\underline{P}')$ implies the conservation of total momentum, we will work from now in the full barycentric frame where $\underline{P}$ is taken to be zero. The $\delta(q_2-q_2')$ factor indicates the conservation of momentum of the bound electron as this is considered to be a spectator particle in the electron-proton interaction. The matrix element $\langle q_{31}|T_2(E)|q_{31}'\rangle$ is the two-body off-shell Coulomb T matrix of particles 1 and 3 in their own two-body centre of mass frame, and we note

that the centre of mass energy E is dependent on the kinetic energy of particle 2 (Ahmadzadeh and Tjon, 1965).

Using Equations (3.7) and (3.5a,b) we obtain for $\langle F | T_2(E) | i \rangle$,

$$\langle F | T_2(E) | i \rangle = \int \cdots \int dq_2\, dq_2'\, dq_{23}\, dq_{23}' \langle F | q_2\, q_{23} \rangle \times$$

$$\times \langle q_2\, q_{23} | T_2(E) | q_2'\, q_{23}' \rangle \langle q_2'\, q_{23}' | i \rangle$$

$$= \int \cdots \int dq_2\, dq_2'\, dq_{23}\, dq_{23}'\, \delta(q_2 - q_F)\, \phi_{1s}^*(q_{23}) \times$$

$$\times\, \delta(q_2 - q_2') \langle q_{23} | T_2\left(E - \frac{q_2^2}{2\mu_2}\right) | q_{23}' \rangle\, \delta(q_2' - q_i)\, \phi_{1s}(q_{23}') \qquad (3.8)$$

The integrations over q_2 and q_2' are trivial leading to the result that $q_2 = q_F$ and $q_2' = q_i$ throughout the remainder of the integrand. To further reduce the number of variables we can express q_2 in terms of q_{23}, q_i and q_F by using relations from Figure (3.2) and the fact that for the $P=0$ barycentric system $q_i = p_i$ $(i=1,2,3)$. We obtain the coordinate relation

$$q_2 = q_{23} - \frac{m_2}{m_2 + m_3}\, q_F \qquad (3.9a)$$

and

$$q_2 - q_2' = q_{23} - q_{23}' + \frac{m_2}{m_2 + m_3}\, \Delta q \qquad (3.9b)$$

where $\Delta q = q_i - q_F = 2|q_i| \sin \theta/2$ is the momentum transfer for elastic scattering through an angle θ. We can therefore perform the integration over q_{23}' and obtain the relation

$$q_{23}' = q_{23} + \frac{m_2}{m_2 + m_3}\, \Delta q \qquad (3.10)$$

The mass of the proton m_3 is of the order of 10^3 times greater than the mass of the electron, $m_2 = m_e$, so we may take the limit $m_3 \to \infty$ without losing substantial accuracy. This limiting process is equivalent to considering the proton to be stationary during the collision, and is a standard approximation for the electron-hydrogen problem. In this limit with the use of Equations (3.8) and (3.10) and the expression for q_3, from Figure (3.2), the matrix element

$\langle F | T_2(E) | i \rangle$ reduces to an integration over one momentum vector,

$\langle F | T_2(E) | i \rangle$

$$= \int dq_2 \, \phi_{1s}^*(q_2) \, \phi_{1s}(q_2) \langle q_F | T_2(E - \frac{q_2^2}{2m_e}) | q_i \rangle \qquad (3.11)$$

The calculation for the electron-electron contribution is similar to the above and the analogue of Equation (3.8) is

$$\langle F | T_3(E) | i \rangle = \int \cdots \int dq_1 \, dq_1' \, dq_{23} \, dq_{23}' \, \delta(q_1 - q_F) \, \phi_{1s}^*(q_{23}) \times \qquad (3.12)$$

$$\times \, \delta(q_3 - q_3') \langle q_{12} | T_3(E - \frac{q_3^2}{2m_3}) | q_{12}' \rangle \, \delta(q_1' - q_i) \, \phi_{1s}(q_{23}')$$

where we now have the coordinate relations

$$q_3 = - \frac{m_3}{m_2 + m_3} \, q_1 - q_{23} \qquad (3.13)$$

Again the integrations over q_1, q_1' and q_{23}' can be performed trivially and in the limit $m_3 \to \infty$ we obtain for $\langle F | T_3(E) | i \rangle$

$\langle F | T_3(E) | i \rangle$

$$= \int dq_{23} \, \phi_{1s}^*(q_3 + q_F) \, \phi_{1s}(q_3 + q_i) \langle q_F + \tfrac{1}{2} q_3 | T_3(E - \frac{q_3^2}{4m_e}) | q_i + \tfrac{1}{2} q_3 \rangle \qquad (3.14)$$

In Equations (3.11) and (3.14) we must substitute the
expressions for the attractive and the repulsive two-
body off-shell Coulomb T matrices respectively. We
have been mainly concerned with the T matrix for
positive energy $\mathcal{E} > 0$, i.e. for the regions $q_2^2 < 2m_e E$
in Equation (3.11) and $q_3^2 < 4m_e E$ in (3.14). For
the remaining regions of $|q_2|$ and $|q_3|$ space we must use
the $\mathcal{E} < 0$ form of the Coulomb T matrix given by
Equations (2.39) and (2.40). For example, Equation (3.11)
must be divided into two integrals

$$\langle F | T_2(E) | i \rangle$$

$$= \int_{0 < |q_2| < (2m_e E)^{1/2}} dq_2 \, \phi_{1s}^*(q_2) \, \phi_{1s}(q_2) \langle q_F | T_2(E > 0) | q_i \rangle \qquad (3.15)$$

$$+ \int_{(2m_e E)^{1/2} \le |q_2| < \infty} dq_2 \, \phi_{1s}^*(q_2) \, \phi_{1s}(q_2) \langle q_F | T_2(E < 0) | q_i \rangle$$

For the scattering problem, where $\mathcal{E} > 0$, it is to be
expected that the second integral is negligible and we
shall ignore this contribution in most of our calculations.
In fact, the insignificance of this integral can be
demonstrated numerically for the physical processes we
consider (Roberts, private communication). The same
arguments hold for $\langle F | T_3(E) | i \rangle$.

We are mostly interested in contributions to $\langle F | T_2(E) | i \rangle$
and $\langle F | T_3(E) | i \rangle$ from the classical path part of
the T matrix, T_c , so in the next section we shall
evaluate $\langle F | T_2^c(E) | i \rangle$ and $\langle F | T_3^c(E) | i \rangle$ where the
c superscript indicates that the classical path term
of the two-body T matrix has been used. In later
sections we shall evaluate contributions from the Born
and pole terms of the T matrix.

3.3 Evaluation of the classical path term

a) the electron-proton term $\langle f|T_2^c(\epsilon)|i\rangle$

The electron-proton contribution to the scattering matrix,
$\langle F|T_2^c(\epsilon)|i\rangle$, is relatively simple to calculate
and reduces to a one-dimensional integral. The inter-
action is attractive so we make use of Equation (2.35)
for T_c . The choice of the factor $g(T,T')$ depends
on the sign of $(T-\epsilon)$ and $(T-\epsilon')$. From Equations (3.4),
(3.6) and (3.7) we have for the electron-proton
interaction,

$$T-\epsilon = \frac{q_{31}^2}{2\mu_{31}} - \left(\frac{q_f^2}{2\mu_1} - \frac{p_0^2}{2\mu_3} - \frac{q_2^2}{2\mu_2}\right) \qquad (3.16)$$

which because of the equivalence of the pairs of
conjugate momentum variables can be written

$$T-\epsilon = \frac{1}{2\mu_{23}}\left(q_{23}^2 + p_0^2\right) \underset{m_3\to\infty}{=} \frac{1}{2m_e}\left(q_{23}^2 + p_0^2\right) \qquad (3.16a)$$

Therefore $(T-\epsilon)$ is positive and we can similarly show
that $(T'-\epsilon)$ is also positive, so that $g(T,T')=1$ must
be chosen in the expression for T_c . We also note that
this implies that the electron-proton paths all lie in
the classically accessible region of momentum space.

Taking the limit $m_3\to\infty$ we therefore have for T_c

$$T_c = \frac{-p_0^3 \exp(i\nu\omega)}{2\pi\nu m_e^3 |\epsilon-T||\epsilon-T'|(1-\exp(-2\pi\nu))\sinh\omega} \qquad (3.17)$$

where from (3.9a) and (3.16a)

$$|\epsilon-T| = |\epsilon-T'| = \frac{1}{2m_e}\left(q_2^2+p_0^2\right) \qquad (3.18)$$

From the definition for ν and ω for attractive scattering we have

$$\nu = \frac{p_o}{\left(2m_e E - q_2^2\right)^{1/2}} \tag{3.19a}$$

and

$$\cosh \omega = 1 + \frac{2(2m_e E - q_2^2)\Delta q^2}{\left(p_o^2 + q_2^2\right)^2} \tag{3.19b}$$

It is apparent that T_c is independent of the angular part of the vector q_2. The ground state hydrogen atom wave functions $\phi_{1s}(q_2)$ in (3.11). are also independent of angle, so the integration over angle can be performed trivially. The momentum representation of the functions $\phi_{1s}(q)$ is given by (Bethe and Salpeter, p.125)

$$\phi_{1s}(q) = \frac{2\sqrt{2}}{\pi} \frac{p_o^{5/2}}{\left(p_o^2 + q^2\right)^2} \tag{3.20}$$

Expressing all quantities in atomic units, that is, momenta in units of the Bohr momentum p_o, and energies in Rydbergs, then we obtain for $\langle F | T_2^c(E) | i \rangle$

$$\langle F | T_2^c(E) | i \rangle = \frac{32}{\pi^2 m_e \Delta q} \int_0^{(E)^{1/2}} \frac{dq \; q^2 \exp(i\nu\omega)}{\left(1+q^2\right)^5 \left(1+\frac{1}{2}z\right)^{1/2}\left(1-\exp(-2\pi\nu)\right)} \tag{3.21}$$

where

$$z = \frac{2(E-q^2)\Delta q^2}{\left(1+q^2\right)^2} \tag{3.22a}$$

and

$$\cosh \omega = 1 + z \tag{3.22b}$$

$$\nu = \frac{1}{\left(E-q^2\right)^{1/2}} \tag{3.22c}$$

b) the electron-electron term $\langle F | T_3^c(E) | i \rangle$

We can see from Equations (3.4), (3.6) and (3.12) that

$$T - \varepsilon = \frac{q_{12}^2}{2\mu_{12}} - \left(\frac{q_F^2}{2\mu_{11}} - \frac{p_0^2}{2\mu_{23}} - \frac{q_3^2}{2\mu_3} \right) \tag{3.24}$$

$$\underset{m_3 \to \infty}{=} \frac{1}{2m_e} \left(q_{23}^2 + p^2 \right) > 0$$

We can similarly show that $(T' - \varepsilon) > 0$ and hence from Equation (2.42) for the repulsive interaction, we must choose $\beta(T, T') = \exp(-2\pi\nu)$. The sign of $(T - \varepsilon)$ and $(T' - \varepsilon)$ implies that the electron-electron paths are solely in the classically inaccessible region of momentum space.

Again expressing all quantities in atomic units we obtain from Equations (2.42) and (3.24) the expression for T_c

$$T_c = \frac{p_0^3 \exp(i\nu\omega) \exp(-2\pi\nu)}{2\pi m_e \Delta q \, (1 + q_{23}^2)^{1/2} (1 + q_{23}'^2)^{1/2} (1 + \frac{1}{2}z)^{1/2}} \frac{1}{1 - \exp(-2\pi\nu)} \tag{3.25}$$

where

$$z = \frac{2(2E - q_3^2)\Delta q^2}{(1 + q_{23}^2)(1 + q_{23}'^2)} \tag{3.26a}$$

$$\cosh\omega = 1 + z \tag{3.26b}$$

and the coordinate relations are

$$q_{23} = q_3 + q_F \tag{3.27a}$$

$$q_{23}' = q_3 + q_i \tag{3.27b}$$

We see from these relations that the electron-electron T matrix is dependent on $\hat{q}_{23}$, and this makes this contribution more difficult to evaluate than the one from the electron-proton interaction. On substitution

of equations (3.20) and (3.25) into (3.14) we obtain

$$\langle F | T_3^c(E) | i \rangle$$

$$= \frac{4}{\pi^3 m_e \Delta q} \int_{0 < |q_3| < (2E)^{1/2}} dq_{23} \frac{\exp(-i\nu w)\exp(-2\pi\nu)}{(1+q_{23}^2)(1+q_{23}'^2)(1+\frac{1}{2}z)^{1/2}(1-\exp(-2\pi\nu))} \qquad (3.28)$$

where

$$\nu = \frac{2}{(2E-q_3^2)^{1/2}} \qquad (3.29)$$

From Equations (3.27) and (3.28) we see that we need to know the angles between q_3 and q_F , and between q_3 and q_i . We are at liberty to choose the orientations of q_i and q_F in momentum space. For convenience we have chosen the polar axis to bisect the scattering angle Θ so that q_i and q_F are coplanar and are aligned as shown in Figure (3.3). Then the angles between the two fixed vectors and q_3 , which has polar angles Θ and ϕ , are given by

$$\cos(q_3, q_i) = -\sin\Theta \sin\phi \sin\Theta/2 + \cos\Theta \cos\Theta/2 \qquad (3.29a)$$

$$\cos(q_3, q_F) = \sin\Theta \sin\phi \sin\Theta/2 + \cos\Theta \cos\Theta/2 \qquad (3.29b)$$

Writing Equation (3.28) more explicitly we now obtain

$$\langle F | T_3^c(E) | i \rangle$$

$$= \frac{4}{\pi^3 m_e \Delta q} \int_0^{2\pi} d\phi \int_0^{\pi} d\Theta \sin\Theta \int_0^{(2E)^{1/2}} \frac{dq_3 \, q_3^2 \exp(-i\nu w)\exp(-2\pi\nu)}{(1+q_{23}^2)^{5/2}(1+q_{23}'^2)^{5/2}(1+\frac{1}{2}z)^{1/2}(1-\exp(-2\pi\nu))} \qquad (3.30)$$
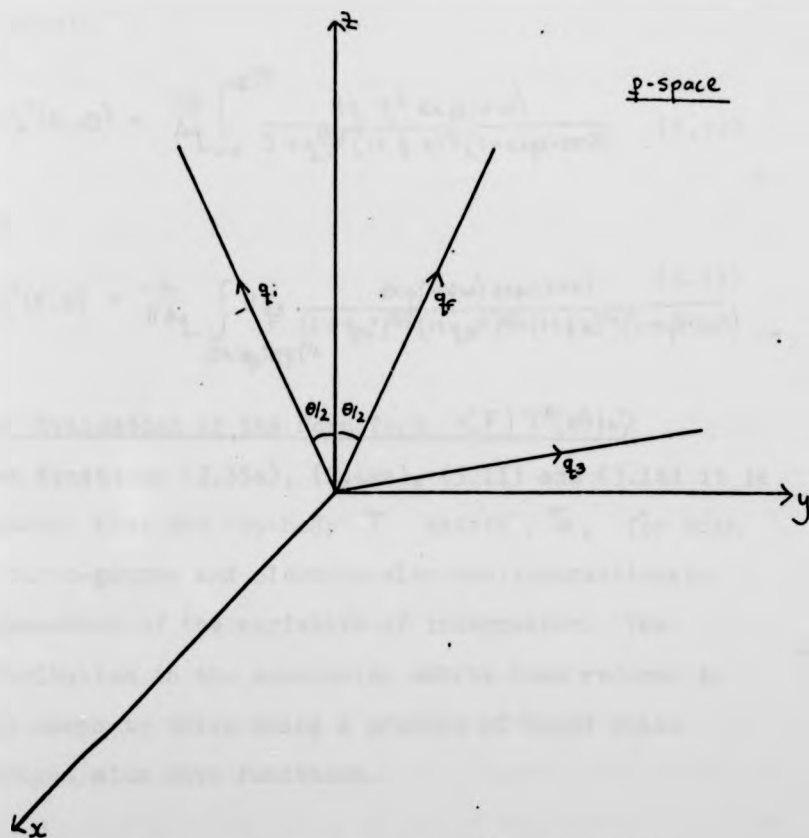
where

$$q_{23}^2 = q_F^2 + q_3^2 + 2 q_3 q_F \cos(q_3, q_F) \qquad (3.31a)$$

and

$$q_{23}'^2 = q_i^2 + q_3^2 + 2 q_3 q_i \cos(q_3, q_i) \qquad (3.31b)$$

FIGURE 3.3

The orientation of the vectors q_i, q_f and q_3.
q_i has polar coordinates $(q_i, 2\pi - \theta/2, 0)$.
q_f has polar coordinates $(q_f, \theta/2, 0)$.
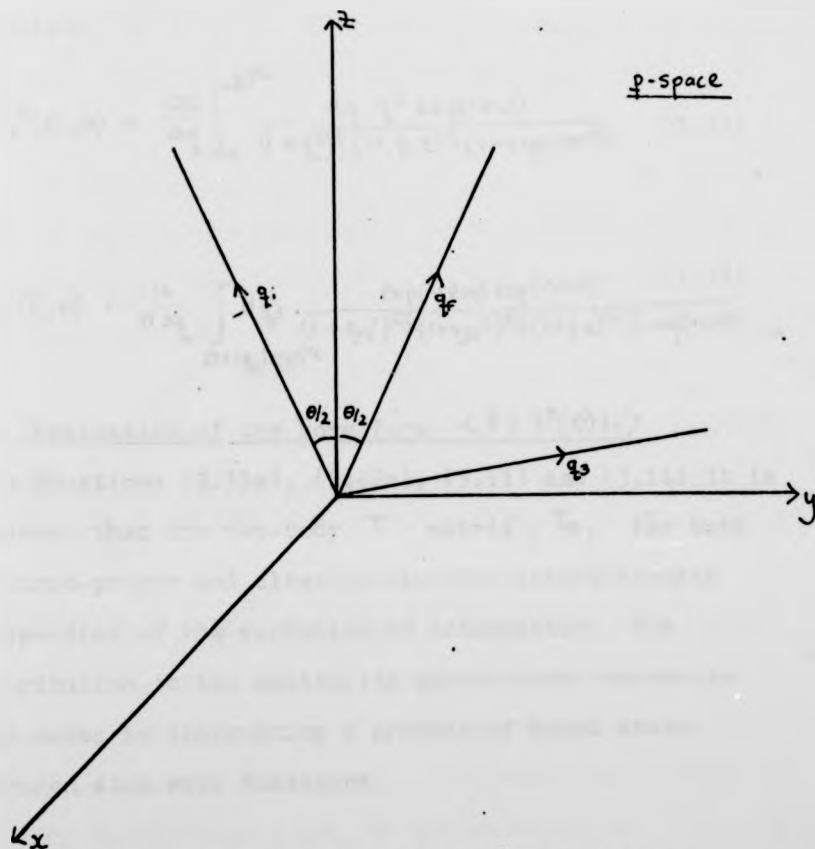q_3 has polar coordinates (q_3, α, ϕ).

FIGURE 33

The orientation of the vectors q_i, q_f and q_3.
q_i has polar coordinates $(q_i, 2\pi - \theta/2, 0)$.
q_f has polar coordinates $(q_f, \theta/2, 0)$.
q_3 has polar coordinates (q_3, α, ϕ).

Finally we express the results for the electron-proton
and electron-electron interactions in terms of their
contributions to the scattering amplitude $F(E,\theta)$.
From Equations (3.2), (3.23) and (3.28), and writing
$F_2^C(E,\theta)$ for the contribution to the scattering
amplitude from the electron-proton classical path term,
we obtain

$$F_2^C(E,\theta) = \frac{128}{\Delta q} \int_0^{(E)^{1/2}} \frac{dq \; q^2 \exp(i\nu\omega)}{(1+q^2)^5 (1+\frac{1}{2}z)^{1/2} (1-\exp(-2\pi\nu))} \quad (3.32)$$

and

$$F_3^C(E,\theta) = \frac{-16}{\pi\Delta q} \int_{0<|q_3|<(E)^{1/2}} dq_3 \frac{\exp(-i\nu\omega) \exp(-2\pi\nu)}{(1+q_{23}^2)^{5/2} (1+q_{23}'^2)^{5/2} (1+\frac{1}{2}z)^{1/2} (1-\exp(-2\pi\nu))} \quad (3.33)$$

3.4 Evaluation of the Born Term $\langle F|T^0(E)|L\rangle$

From Equations (2.35a), (2.42a), (3.11) and (3.14) it is
apparent that the two-body T matrix , T_B, for both
electron-proton and electron-electron interactions is
independent of the variables of integration. The
contribution to the scattering matrix then reduces in
both cases to integrating a product of bound state
hydrogen atom wave functions.

For the electron-proton case we have

$$\langle F|T_2^0(E)|L\rangle = \frac{-\rho^2}{2\pi^2 \mu_{13} \Delta q^2} \int dq \; \phi_{1s}^*(q) \, \phi_{1s}(q) \quad (3.34)$$

We have argued,(Equation 3.15),that the limits on the
integration over $|q|$ should be $0<|q|<(E)^{1/2}$. The
integrand in (3.34) is proportional to q^{-6} , so in
fact for all but the lowest energies, contributions from
the region $(E)^{1/2}<|q|<\infty$ will be insignificant.

However by extending the upper limit of integration to infinity in Equation (3.34) we are able to perform the integration analytically without changing the result. We obtain

$$f_2^B(E, \theta) = \frac{2}{\Delta q^2} \qquad (3.35)$$

where $f_2^B(E, \theta)$ is the contribution to the scattering amplitude from the electron-proton Born term of the T matrix.

This is exactly the same result as a standard first Born calculation of the contribution to the scattering amplitude from the electron-proton interaction.

The Born term of the T matrix for the electron-electron interaction gives the following contribution to the scattering matrix

$$\langle F | T_3^B(E) | i \rangle = \frac{P_c}{2\pi^2 \mu_{12} \Delta q^2} \int dq_{23} \, \phi_{1s}^*(q_3 + q_f) \, \phi_{1s}(q_3 + q_i) \quad (3.36)$$

Using the same arguments as in the previous calculation we can extend the limits of the integration to all $|q_3|$ space, and though the integral is slightly more difficult than in the previous case, it can be evaluated analytically (see Appendix) to give

$$f_3^B(E, \theta) = \frac{-32}{\Delta q^2 (\Delta q^2 + 4)^2} \qquad (3.37)$$

This again is the same result as that given by the first Born approximation. Thus, using the derived

form of the two-body off-shell Coulomb T matrix in
the first order iterate of the Faddeev equations
demonstrates explicitly that the latter contain the
first Born approximation for the elastic $e-H$
scattering problem.

Summing Equations (3.35) and (3.37) we obtain the total
contribution to the scattering matrix from the Born
term of the two-body T matrix.

$$f_B(E,\theta) = \frac{2(\Delta q^2 + 8)}{(\Delta q^2 + 4)^2} \qquad (3.38)$$

3.5 Evaluation of the pole terms

From the expressions for the two-body off-shell Coulomb
T matrix we see that the pole term is in fact an
infinite sum of contributions. On the energy shell
only the $n=0$ term contributes, so we shall initially
calculate this term.

We already know, from our calculations of the classical
path contributions, the sign of the factors $(E-T)$ and
$(E-T')$, so we can infer that for both attractive and
repulsive interactions the factor $\xi = sign\ (E-T)(E-T')$
is positive . In fact it is apparent from Equations
(2.35b) and (2.42b) that the pole terms for the attractive
and repulsive interactions differ only by sign and mass
factors.

BR

a) the electron-proton term $\langle F|T_2^{p}(E)|i\rangle$

The analysis is much the same as for the classical
path term and we shall just quote the result for
$\langle F|T_2^{p(o)}(E)|i\rangle$, the zero order pole term for the
electron-proton interaction

$$\langle F|T_2^{p(o)}(E)|i\rangle = \frac{16}{\pi^3 m_e \Delta q} \int_0^{(E)^{1/2}} \frac{dq \; q^2 (E-q^2)^{1/2}}{(q^2+1)^5 (1+\frac{1}{2}z)^{1/2}} \quad (3.39)$$

where z is defined by (3.22a). The analysis is simply
extended to include all orders of the pole term. We note
from Equation (2.35b) that for $\epsilon_i = 1$, the contribution
from $n = -1$ is equal to the contribution from $n = 1$.
Thus, the nth order pole term (where n can be positive
or negative) is given by

$$\langle F|T_2^{p(n)}(E)|i\rangle$$

$$= \frac{16}{\pi^3 m_e \Delta q} \int_0^{(E)^{1/2}} \frac{dq \; q^2 (E-q^2)^{1/2}}{(q^2+1)^5 (1+\frac{1}{2}z)^{1/2} \left[n^2(E-q^2)+1\right]\left[1+z+(z(z+2))^{1/2}\right]^{|n|}} \quad (3.40)$$

b) the electron-electron term $\langle F|T_3^{p}(E)|i\rangle$

Again this calculation is more difficult than the one for
the electron-proton contribution, however utilising the
results of the classical path electron-electron
calculation we may write down the analogues of equations
(3.39) and (3.40)

$$\langle F|T_3^{p(o)}(E)|i\rangle$$

$$= \frac{-1}{\pi^4 m_e \Delta q} \int_{0 < q_{23} < (2E)^{1/2}} dq_3 \frac{(2E-q_3^2)^{1/2}}{(1+q_{23}^2)^{5/2}(1+q_{23}'^2)^{5/2}(1+\frac{1}{2}z)^{1/2}} \quad (3.41)$$

where $q_{23}^2, q_{23}'^2$ and z are defined by (3.31a), (3.31b)
and (3.26a) respectively.

$$\langle F|T_3^{p(n)}(E)|i\rangle$$

$$= \frac{-4}{\pi^4 m_e \Delta q} \int dq_3 \frac{(2E-q_3^2)^{1/2}}{(1+q_{23}^2)^{5/2}(1+q_{23}'^2)^{5/2}(1+\frac{1}{2}z)^{1/2}\left[n^2(2E-q^2)+4\right]} \quad (3.42)$$

$$\times \frac{1}{\left[1+z+(z(z+2))^{1/2}\right]^{|n|}}$$

We therefore obtain for the contributions to the scattering amplitude from the nth order pole terms

$$F_2^{P(n)}(E,\theta)$$

$$= \frac{-64}{\pi \Delta_q} \int_0^{(E)^{1/2}} \frac{dq \; q^2 (E-q^2)^{1/2}}{(1+q^2)^5 (1+\frac{1}{2}z)^{1/2} \left[n^2(E-q^2)+1\right]\left[1+z+(z(z+2))^{1/2}\right]^n} \quad (3.43)$$

and

$$F_3^{P(n)}(E,\theta)$$

$$= \frac{16}{\pi^2 \Delta_q} \int dq_3 \frac{(2E-q_3^2)^{1/2}}{(1+q_{23}^2)^{5/4}(1+q_{23}'^2)^{5/2}(1+\frac{1}{2}z)^{1/2}\left[n^2(2E-q^2)+4\right]} \times \frac{1}{\left[z+1+(z(z+2))^{1/2}\right]^n} \quad (3.44)$$

Before quoting the results for the calculations of $F^B(E,\theta)$, $F^P(E,\theta)$ and $F^C(E,\theta)$, we note that the pole terms and Born terms are purely real, whilst the classical path term has a complex part. Thus the complex part of the scattering amplitude is obtained solely from contributions from the classical path terms. We obtain the total contribution for each of the three terms by summing the contributions from the electron-proton and electron-electron interactions, the real and imaginary parts being summed separately for the classical path term.

3.6 Calculations and Results

The Born contribution to the scattering amplitude has been evaluated analytically. Unless we make further approximations the pole terms and the classical path term must be evaluated numerically. For both of these terms the electron-proton contribution is a one-dimensional integral whilst the electron-electron contribution involves a more difficult three-dimensional integration. We shall firstly evaluate the various orders of the pole term and compare

the contributions to the scattering amplitude with those obtained from the Born term. We may therefore examine whether the on-shell correspondence identity is being approached.

a) The Pole and Born terms

On examination of the integrands of Equations (3.39) - (3.41) at high energies it is apparent that the majority of the contributions to the integrals come from small q or $|q_3|$. This would indicate that the on-shell limit is being approached since for example, this limit is given for the electron-proton interaction by

$$\frac{q_3^2}{2M_3} \sim \frac{q_F^2}{2m_e} \longrightarrow \frac{q_F^2}{2m_e} - \frac{p_0^2}{2m_e} - \frac{q^2}{2M_2} \qquad (3.45)$$

At high energies $q_F^2 \gg p_0^2$, and hence the on-shell limit is approached when q is small. A similar argument holds for the electron-electron interaction.

The integrations in Equations (3.39) and (3.40) are performed using a subroutine RKMER4 of Banks. One half a second of processing time is taken on the Elliott 4130 at Stirling to provide a result for the scattering amplitude at one energy and one angle. The electron-electron interaction integrals are performed by using the RKMER4 routine twice and a Gaussian method for the ϕ integration, the integrands being a slowly varying function of the azimuthal angle. The time to achieve one result is much longer, being of the order of one and a half minutes.

In Figures (3.4) and (3.5) we compare the contributions
to the scattering amplitude from the $n=0$ pole term
with that from the $n=\pm 1$ pole terms at energies of 200ev
and 1kev, and at scattering angles between 5° and 90°.
At 200ev and 5° scattering angle the contribution from
the first order terms is approximately 1% of the
contribution from the zeroth order pole term, this
percentage decreasing rapidly with increasing angle.
For scattering at 1kev the value of the contributions
from the $n=\pm 1$ terms relative to those from the $n=0$
term is even less than the 200ev case at all angles of
scattering. Thus for energies greater than 200ev,
contributions from the First order pole term are
negligible in comparison with the zeroth order
contribution, an effect which increases with increasing
energy. This effect is evidence that the on-shell limit
is being approached at high energies. By examination
of Equations (3.40) and (3.42) it is evident that
contributions from the $n=\pm 2$ pole terms will be less
than those from the $n=\pm 1$ terms. We shall therefore
neglect all but the zeroth order pole term in our
calculations.

In Figures (3.6) and (3.7) we compare the contributions
to the scattering amplitude from the zero order pole
term with those from the Born term. At an energy of
200ev for scattering angles below 30° there is no evidence
of cancellation of the Born and pole contributions.
However at scattering angles above 30° the percentage
difference between the magnitudes of $f^{B}(E,\theta)$ and $f^{P}(E,\theta)$

FIGURE 3.4

ANGLE	POLE (N = 0)		POLE (N = +1) + POLE (N = -1)	
	$e^- - p^+$	$e^- - e^-$	$e^- - p^+$	$e^- - e^-$
5°	-10.30	2.30	-0.368	0.319
10°	-3.53	0.667	-0.568(-1)	0.480(-1)
20°	-1.03	0.113	-0.673(-2)	0.475(-2)
30°	-0.483	0.273(-1)	-0.183(-2)	0.988(-3)
40°	-0.281	0.828(-2)	-0.732(-3)	0.292(-3)
50°	-0.186	0.301(-2)	-0.363(-3)	0.108(-3)
60°	-0.134	0.128(-2)	-0.209(-3)	0.470(-4)
70°	-0.102	0.614(-3)	-0.133(-3)	0.232(-4)
80°	-0.813(-1)	0.330(-3)	-0.914(-4)	0.127(-4)
90°	-0.673(-1)	0.194(-3)	-0.669(-4)	0.759(-5)

Contributions to the scattering amplitude in atomic
units from the N = 0 and N = ±1 pole terms at
incident energy $\dot{E}$ = 200 ev.
Integer in parenthesis indicates appropiarte power of 10.

FIGURE 3.5

ANGLE	POLE (N=0)		POLE (N=+1) + POLE (N=-1)	
	$e^- - p^+$	$e^- - e^-$	$e^- - p^+$	$e^- - e^-$
5°	-3.39	0.643	-0.237(-2)	0.379(-2)
10°	-0.881	0.891(-1)	-0.201(-3)	0.219(-3)
20°	-0.224	0.525(-2)	-0.161(-4)	0.111(-4)
30°	-0.101	0.702(-3)	-0.370(-5)	0.192(-5)
40°	-0.581(-1)	0.149(-3)	-0.134(-5)	0.505(-6)
50°	-0.380(-1)	0.450(-4)	-0.623(-6)	0.174(-6)
60°	-0.272(-1)	0.165(-4)	-0.341(-6)	0.722(-7)
70°	-0.207(-1)	0.779(-5)	-0.210(-6)	0.363(-7)
80°	-0.165(-1)	0.370(-5)	-0.141(-6)	0.193(-7)
90°	-0.136(-1)	0.220(-5)	-0.101(-6)	0.113(-7)

Contributions to the scattering amplitude in atomic units from the N=0 and N=±1 pole terms at incident energy E = 1 keV.
Integer in parenthesis indicates appropiarte power of 10.

FIGURE 3.6

ANGLE	POLE(N=0)	BORN
5°	-8.00	0.960
10°	-2.86	0.854
20°	-0.920	0.586
30°	-0.456	0.379
40°	-0.273	0.251
50°	-0.183	0.176
60°	-0.133	0.130
70°	-0.101	0.100
80°	-0.810(-1)	0.807(-1)
90°	-0.671(-1)	0.677(-1)

Contributions to the scattering amplitude in atomic units from the N=0 pole term and the Born term at incident energy E = 200ev. Integer in parenthesis indicates appropiarte power of 10.

FIGURE 3.7

ANGLE	POLE (N=0)	BORN
5°	-2.65	0.823
10°	-0.792	0.527
20°	-0.219	0.204
30°	-0.100	0.987(-1)
40°	-0.560(-1)	0.515(-1)
50°	-0.380(-1)	0.379(-1)
60°	-0.272(-1)	0.271(-1)
70°	-0.207(-1)	0.206(-1)
80°	-0.164(-1)	0.164(-1)
90°	-0.136(-1)	0.136(-1)

Contributions to the scattering amplitude in
atomic units from the N=0 pole term and the
Born term · at incident E = 1 keV.
Integer in parenthesis indicates appropiarte
power of 10.

is never greater than 20% reducing rapidly as the angle
increases so that the contributions almost cancel at
90° scattering angle. At 1kev this percentage
difference is smaller than that at 200ev for all
scattering angles. Henceforth we shall ignore
contributions from the pole and Born terms for $E \geqslant 200ev$
and $\theta \geqslant 30°$, an approximation which is very good
for a large part of this range and still good for lower
energies and angles. The cancellation of the pole and
Born contributions is a further indication that the
on-shell limit is approached at high energies.

Thus, for the angle and energy range defined, we can to
a good approximation express the scattering amplitude,
and therefore the differential cross section, in terms
of the classical path part of the T matrix. The
on-shell correspondence identity is being satisfied and
a physical explanation of this phenomena can be obtained
from consideration of a classical picture of the collision
process as follows.

At high energies the electron velocity is large and the
time of interaction between the electron and the atom is
short compared with the period of rotation of the bound
electron around the nucleus. We can assume that for
large angles of scattering the electron has passed close
to the nucleus, (i.e. the impact parameter is small), and
the effect of the bound electron is small. In fact the

effect of the bound electron is a small perturbation
of the two-body Rutherford scattering process and a
correspondence identity is known to exist for the
latter (Norcliffe et.al., 1969b). For low angles of
scattering the impact parameter is large, contributions
from the electron-electron interaction become important,
and the Rutherford scattering identity no longer holds.
The electron-electron interaction is also important at
low energies when the period of the bound electron is
much shorter than the interaction time. Therefore, in
the region of scattering we have defined, which is close
to the on-shell region for elastic e-H collisions, the
Rutherford correspondence identity is approached and the
scattering amplitude can be expressed in terms of classical
paths. For lower energies and angles of scattering,
quantal and three-body effects are important (viz. the
pole and Born terms) and the scattering amplitude cannot
be expressed so simply.

b) The Classical Path Term

The computational procedure for calculating the classical
path terms is similar to that used to obtain the pole
terms. Again the electron-proton single integral given
by equation (3.32) can be evaluated relatively simply
and quickly, whilst the electron-electron contribution
proves more difficult to compute. Both terms contribute
real and complex parts to the scattering amplitude. The
angular distributions of the contributions are shown for
two-energies in Figures (3.8) and (3.9).

FIGURE 3.8

ANGLE	$e^- \cdot e^-$ part		$e^- \cdot p^+$ part	
	REAL	IMAG	REAL	IMAG
5°	-0.162	0.172	0.198(+2)	0.859(+1)
10°	-0.188(-1)	0.640(-1)	0.578(+1)	0.459(+1)
20°	0.152(-2)	0.112(-1)	0.118(+1)	0.180(+1)
30°	0.645(-3)	0.268(-2)	0.371	0.935
40°	0.196(-3)	0.839(-3)	0.134	0.570
50°	0.659(-4)	0.320(-3)	0.458(-1)	0.355
60°	0.228(-4)	0.141(-3)	0.769(-2)	0.278
70°	0.836(-5)	0.700(-4)	-0.499(-2)	0.212
80°	0.326(-5)	0.386(-4)	-0.185(-1)	0.168
90°	0.124(-5)	0.232(-4)	-0.226(-1)	0.138

Contributions to the scattering amplitude in atomic
units from the classical path term at incident
energy E = 200ev.
Integer in parenthesis indicates appropiarte power of 10.

FIGURE 3.9

ANGLE	e⁻-e⁻ part		e⁻-p⁺ part	
	REAL	IMAG	REAL	IMAG
5°	-0.170	0.224	2.22	4.78
10°	-0.176(-1)	0.362(-1)	1.24	1.98
20°	-0.692(-3)	0.197(-2)	0.221	0.226
30°	-0.137(-3)	0.277(-3)	0.898(-1)	0.111
40°	-0.307(-4)	0.535(-4)	0.472(-1)	0.669(-1)
50°	-0.971(-5)	0.164(-4)	0.287(-1)	0.453(-1)
60°	-0.382(-5)	0.602(-5)	0.192(-1)	0.333(-1)
70°	-0.175(-5)	0.296(-5)	0.138(-1)	0.257(-1)
80°	-0.907(-6)	0.133(-5)	0.104(-1)	0.202(-1)
90°	-0.541(-6)	0.804(-6)	0.623(-2)	0.173(-1)

Contributions to the scattering amplitude in atomic
units from the classical path term at incident
energy E = 1kev.
Integer in parenthesis indicates appropiarte power of 10.

For scattering angles above 30° the contributions from
the electron-electron interaction are negligible. This
is in accordance with the arguments in the last paragraph
of Section 3.6a. In later calculations it shall be
convenient to neglect the electron-electron contributions,
though we retain them for completeness in this section.

The differential cross section is found by taking the
modulus square of the scattering amplitude. Our results
for $d\sigma/d\Omega$ for elastic e-H scattering are shown by
curve 1 of Figures (3.10) and (3.11), where a comparison
is made with the results obtained using a standard first
Born approximation calculation.

At E = 200ev the discrepancy between the Born result and
the classical path result is large. For scattering angles
less than 30° the Born differential cross section approaches
a constant at zero angle, whereas the classical path result
peaks sharply. In fact, as we shall see, the classical
path differential cross section is divergent at zero angle
scattering. Above 30° scattering angle although the
angular distributions predicted by the two theories are
similar, the classical path differential cross section
is considerably larger than the Born. At 1kev scattering
the angular distributions are similar to those at 200ev,
however for large angle scattering the magnitude of the
Born and the classical path results are closer though
by no means equal.
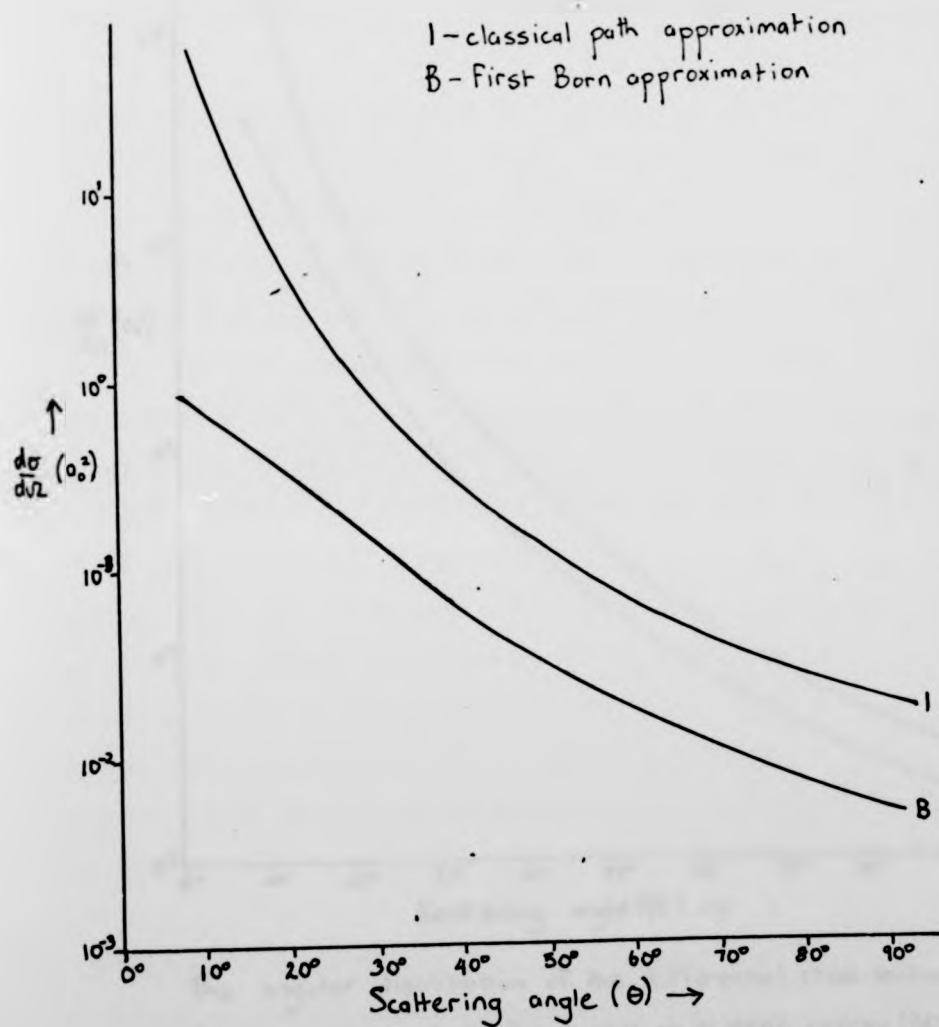
FIGURE 3.10

1 - classical path approximation
B - First Born approximation

The angular distribution of the differential cross section for the collision $e^- + H(1s) \rightarrow e^- + H(1s)$ at incident energy 200ev.
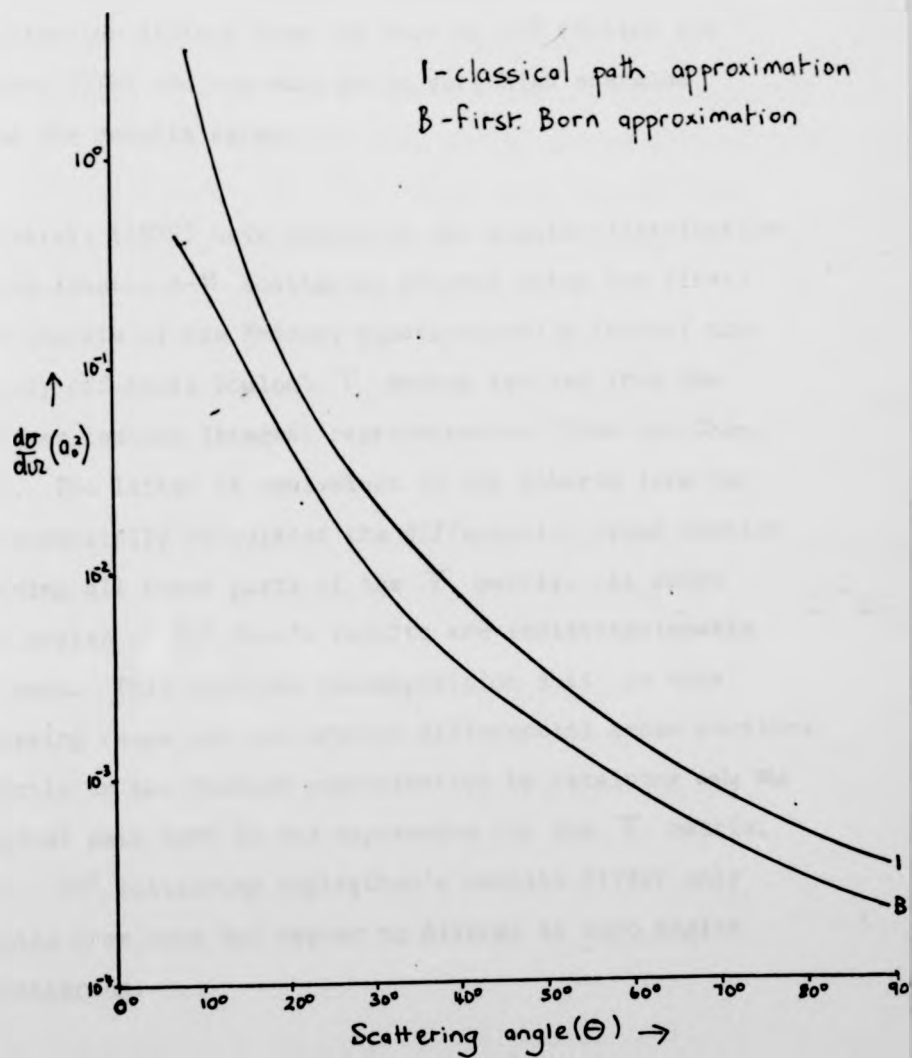
FIGURE 3.11

The angular distribution of the differential cross section for the collision $e^- + H(1s) \rightarrow e^- + H(1s)$ at incident energy 1 keV.

At energies higher than 1kev we can show both numerically
and analytically that the classical path differential
cross section approaches the Born for all but small
angles. However, at 1500ev the classical path
approximation differs from the Born by 40% (Hutton and
Roberts, 1972) and one must go to very high energies
before the results agree.

Chen et.al. (1972) have evaluated the angular distribution
for the elastic $e-H$ scattering process using the first-
order iterate of the Faddeev equations and a form of the
two-body off-shell Coulomb T matrix derived from the
Schwinger contour integral representation (Chen and Chen,
1972). The latter is equivalent to the Roberts form but
Chen essentially calculates the differential cross section
retaining all three parts of the T matrix. At 200ev
above angles of 30° Chen's results are indistinguishable
from ours. This confirms the supposition that in this
scattering range one can predict differential cross sections
correctly in the Faddeev approximation by retaining only the
classical path term in the expression for the T matrix.
Below 30° scattering angles Chen's results differ only
slightly from ours and appear to diverge at zero angles
of scattering.

Chen compares his results with the relative experimental
measurements of Teubner et.al. (unpublished) and a
Glauber approximation result (Tai et.al., 1969). The
angular distribution agrees with the experimental
findings over much of the range, but of course the same

agreement is found between the Born calculation and the
renormalized experimental results. A lack of absolute
experimental measurements at 200ev make it impossible
to verify conclusively the magnitude of the differential
cross section, though recent absolute measurements for
50ev $e-H$ elastic scattering (Teubner et.al., 1973) seem
to suggest that the Born approximation gives the more
accurate prediction. Above 30° scattering the Born and
Glauber results are identical. Recent work by Chen
(Chen et.al., 1973) shows that in the second order
iterate of the Faddeev equations for elastic $e-H$
scattering, the differential cross section reduces
to the Glauber result.

In Figure (3.12) we present a distribution of the
differential cross section as a function of energy at
a fixed scattering angle. Choosing $\Theta = 60^{\circ}$ we can
ignore contributions from the electron-electron
interaction so that the differential cross section is
calculated from the classical path electron-proton part
of the T matrix only. The energy dependence of the
differential cross section calculated from the classical
path approximation is seen to be similar to the Born
distribution, and in the high energy limit there is
a slow convergence of the former result on the latter.
From our results and Chen's we conclude that only for
very high energies do differential cross sections
calculated from the first order Faddeev equations tend to
the first Born approximation result.

FIGURE 3.12

I - classical path approximation
B - First Born approximation
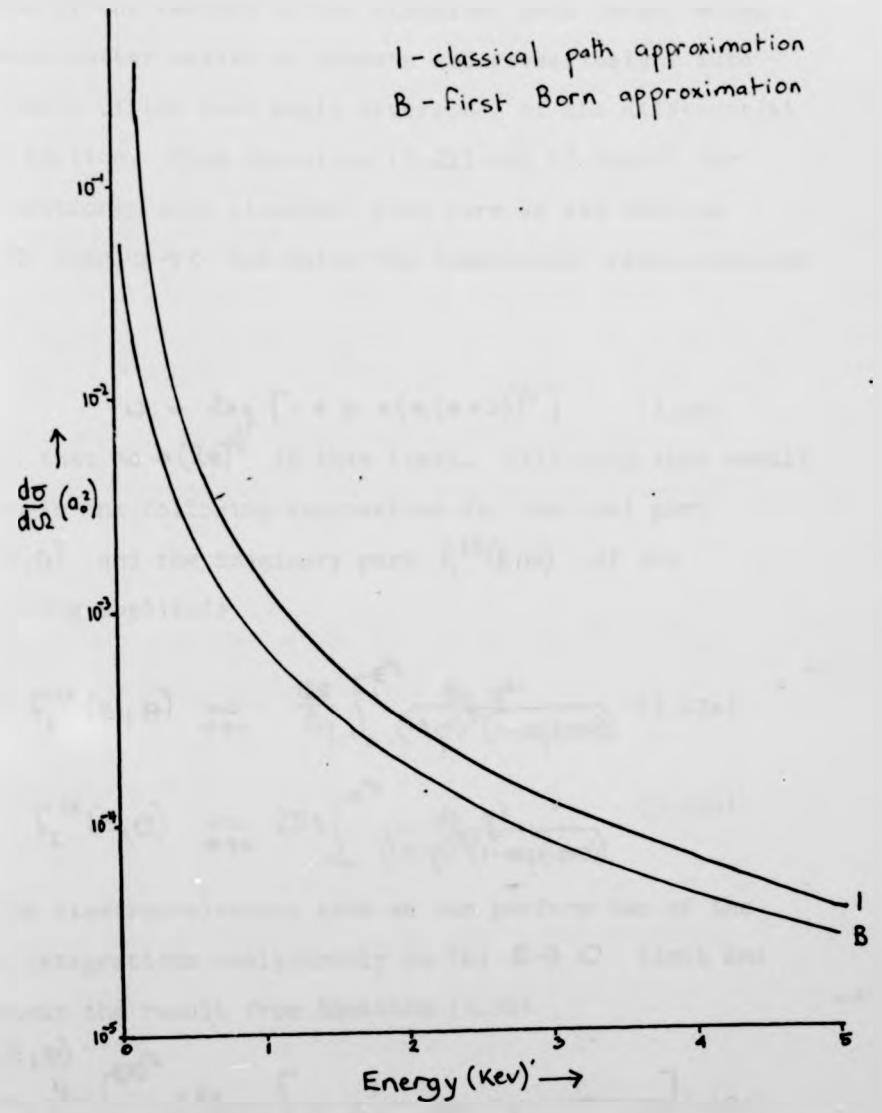
Energy distribution of the differential cross section for the collision $e^- + H(1s) \rightarrow e^- + H(1s)$ at fixed angle of scattering $60°$.

c) Zero angle calculations

As the scattering angle approaches zero we can approximate
several of the factors in the classical path terms, which
makes the latter easier to compute and gives insight into
the source of the zero angle divergence of the differential
cross section. From Equations (3.21) and (3.22a,b) for
the electron-proton classical path term we see that as
$\theta \to 0$ then $z \to 0$ and using the logarithmic representation
of ω,

$$\omega = \log \left[1 + z + (z(z+2))^{1/2} \right] \qquad (3.46)$$

we see that $\omega \to (2z)^{1/2}$ in this limit. Utilising this result
we obtain the following expressions for the real part
$f_2^{CR}(E,\theta)$ and the imaginary part $f_2^{CI}(E,\theta)$ of the
scattering amplitude

$$f_2^{CR}(E,\theta) \underset{\theta \to 0}{=} \frac{128}{\Delta q} \int_0^{E^{1/2}} \frac{dq \; q^2}{(1+q^2)^5 (1-\exp(-2\pi v))} \qquad (3.47a)$$

and

$$f_2^{CI}(E,\theta) \underset{\theta \to 0}{=} 256 \int_0^{E^{1/2}} \frac{dq \; q^2}{(1+q^2)^6 (1-\exp(-2\pi v))} \qquad (3.48b)$$

For the electron-electron term we can perform two of the
three integrations analytically in the $\theta \to 0$ limit and
we obtain the result from Equation (3.30)

$$f_3^{CR}(E,\theta) = \frac{4}{q_i \Delta q} \int_0^{(2E)^{1/2}} \frac{q \, dq}{(\exp(2\pi v)-1)} \left[\frac{1}{\{1 + (q+q_i)^2\}^4} - \frac{1}{\{1 + (q-q_i)^2\}^4} \right] \quad 3.49a)$$

$$f_3^{CI}(E,\theta) \qquad\qquad\qquad\qquad\qquad (3.49b)$$
$$= \frac{12.8}{q_i} \int_0^{(2E)^{1/2}} \frac{q \, dq}{(\exp(2\pi v)-1)} \left[\frac{1}{\{1 + (q-q_i)^2\}^5} - \frac{1}{\{1 + (q+q_i)^2\}^5} \right]$$

From these results we see that in both cases the real part of the scattering amplitude diverges as $(\Delta q)^{-1}$, $(\Delta_L = 2q_i \sin \theta/2$ for elastic collisions), whereas the imaginary part is finite at zero angles. Numerical calculations on the above results give the same values for the zero angle differential cross section as calculations performed at small scattering angles $(\sim 0.1^{\circ})$ using the general form of the classical path term. This is a valuable check on the correctness of our computational procedure. It is also of note that $f_2^{CR}(E, \theta)$ and $f_2^{CR}(E, \theta)$ are of opposite sign at small angles which leaves the possibility that the zero angle divergences in the scattering amplitude may cancel.

We have mentioned that we do not expect the classical path term to provide good results at small angles of scattering. It is more interesting to examine the behaviour of the contributions from the full T matrix, including the $\mathcal{E} < 0$ T matrix, at zero angles. Taking the zero angle limit $\omega \to 0$ of the factor representing the sum of the pole and classical path terms we obtain

$$\left[\frac{1}{2} \sum_{n=-\infty}^{\infty} \frac{e^{-|n|\omega}}{n^2 + \nu^2} - \frac{\pi \exp(i\nu\omega)}{\nu(1 - \exp(-2\pi\nu))} \right] \xrightarrow[\theta \to 0]{} \frac{-\pi}{2\nu} \qquad (3.50)$$

In the same way $\chi \to 0$ in the zero angle limit and we obtain for $\langle f | T_2(E) | i \rangle$ a sum of three terms

$$\langle f | T_2(E) | i \rangle \xrightarrow[\theta \to 0]{} \langle f | T_2^{BO} | i \rangle$$

$$+ \frac{p_0^2}{2\pi m_e \Delta q} \left[\int_{E^{1/2} \leq |q| < \infty} \frac{d^3q \, |\phi(q)|^2}{(1 + q^2)} - \int_{0 < |q| < E^{1/2}} \frac{d^3q \, |\phi(q)|^2}{1 + q^2} \right] \qquad (3.51)$$

where $\langle F | T_2^{BO} | i \rangle$ is the Born term at zero scattering angle, and the second and third terms come from the $\varepsilon < 0, \varepsilon > 0$ T matrix respectively. For the electron-electron interaction we have in the zero angle limit

$$\langle F | T_3(E) | i \rangle = \langle F | T_3^{BO} | i \rangle$$
$$- \frac{p_0^2}{2\pi m_e \Delta q} \left[\int_{(2E)^{1/2} \leq |q| < \infty} \frac{d^3q \, |\phi(q)|^2}{1+q^2} + \int_{0 < |q| < E^{1/2}} \frac{d^3q \, |\phi(q)|^2}{1+q^2} \right] \quad (3.52)$$

Since $\langle F | T_3^{BO} | i \rangle + \langle F | T_2^{BO} | i \rangle$ is finite in the zero angle limit then the three-body T matrix is given by

$$\langle F | T(E) | i \rangle = \text{const.} - \frac{p_0^2}{\pi m_e \Delta q} \int_{\alpha < |q| < E^{1/2}} \frac{d^3q \, |\phi(q)|^2}{1+q^2} \quad (3.53)$$

Therefore the scattering amplitude diverges as $(\Delta q)^{-1}$ at zero scattering angles. In physical reality this of course is not true, and it appears that the zero angle divergence of the differential cross section for elastic scattering is inherent in the Faddeev approximation because of the long range nature of the Coulomb potential. Chen and Sinfailam (1972) also obtain a zero angle divergence for elastic $e-H$ scattering, although they have not included the effect of the $\varepsilon < 0$ T matrix, and attribute this to the same cause (Chen, private communication).

We note from Equations (3.51) and (3.52) that a change of sign in one term would cause the cancellation of the $(\Delta q)^{-1}$ divergence. In a previous note (Hutton and Roberts, 1972, heareafter referred to as Paper II),

it was stated that by altering the $g(T_1 T')$ factor in Equation (2.35c) for the electron-proton interaction, cancellation of the $(\Delta_q)^{-1}$ singularity could be obtained. This is inconsistent and incorrect. The $g(T_1 T')$ factors are uniquely defined in the formalism and even if the reasons given for changing $g(T_1 T'$ (viz. that the value of the factor $g(T_1 T')$ depends on the normalisation of the Coulomb distorted spherical wave associated with $\widetilde{G}_0^{(+)}$, see Chapter 2 page 30) were valid, then to be consistent $g(T_1 T')$ would have to be changed for the repulsive interaction so that the divergence would not be cancelled.

In Paper II we presented results for the differential cross section obtained by taking different $g(T_1 T')$ factors in Equation (3.32). We demonstrated that the magnitude of the differential cross section is strongly dependent on which value of $g(T_1 T')$ is used, apart from in the high energy limit when all three factors give results which converge on the Born. Re-examination of the derivation of the $g(T_1 T')$ factors has confirmed that the value used in Equation (3.32) is correct and that the results presented in Figure (3.9) are the true value of the differential cross section obtained from the first order iterate of the Faddeev equations for the process considered. The discrepancy between the magnitudes of the differential cross sections given in the first order Born and Faddeev methods at large scattering angles is real and due to the

fact that important contributions are contained in the
second order Faddeev term (Chen et.al., 1973). The
zero angle divergence of the differential cross section
is a non-physical property associated with the long
range nature of the Coulomb potential.

c) High energy limit

At high energies ($E \gtrsim 1 kev$) and scattering angles above
10° the electron-electron classical path contribution is
small and we can express the scattering amplitude solely
in terms of the electron-proton contributions. In the
high energy limit we know that the major contribution
to the integral in Equation (3.32) comes from small q
and we may write

$$f_2^c(E, \theta) \underset{E \to \infty}{=} \frac{64}{\pi \Delta q^2} \int_0^\infty \frac{dq \, q^2}{(1+q^2)^4} \exp(i v w) \tag{3.54}$$

In the high energy limit vw is independent of q and
may be written

$$vw \underset{E \to \infty}{=} E^{-1/2} \log(1 + 2E \, \Delta q^2) \tag{3.55}$$

Thus vw approaches zero slowly in the limit $E \to \infty$ for
non-zero scattering angles, and in this limit the
scattering amplitude reduces to a real function which is
equal to the first Born result.

$$f_2^c(E, \theta) \underset{E \to \infty}{=} \frac{2}{\Delta q^2} = f_2^B(E, \theta) \tag{3.56}$$

According to Norcliffe et.al. (1969) ∇w is the classical
action function in units of $\hbar$ along, in this case, a
path joining the vectors q_i and q_f. We can assume
then that the classical action must approach zero in the
high energy limit. From Equation (2.38) we see that the
action along the path between the fixed vectors q_i
and q_f, $S_{fi} \approx r_0 \Delta q$ where r_0 is the distance
of closest approach. It is a well known result of
classical mechanics that for hyperbolic orbits the
distance of closest approach $r_0 \propto q_i^{-2}$. Therefore the
action S_{fi} is proportional to q_i^{-1} and at high
energies and fixed scattering angles S_{fi} tends to
zero. We infer that the slow convergence of the first
order Faddeev result on the Born, is in part associated
with the action along the classical paths slowly
approaching zero in the high energy limit. We assume
that the second order Faddeev calculations of Chen et.al.
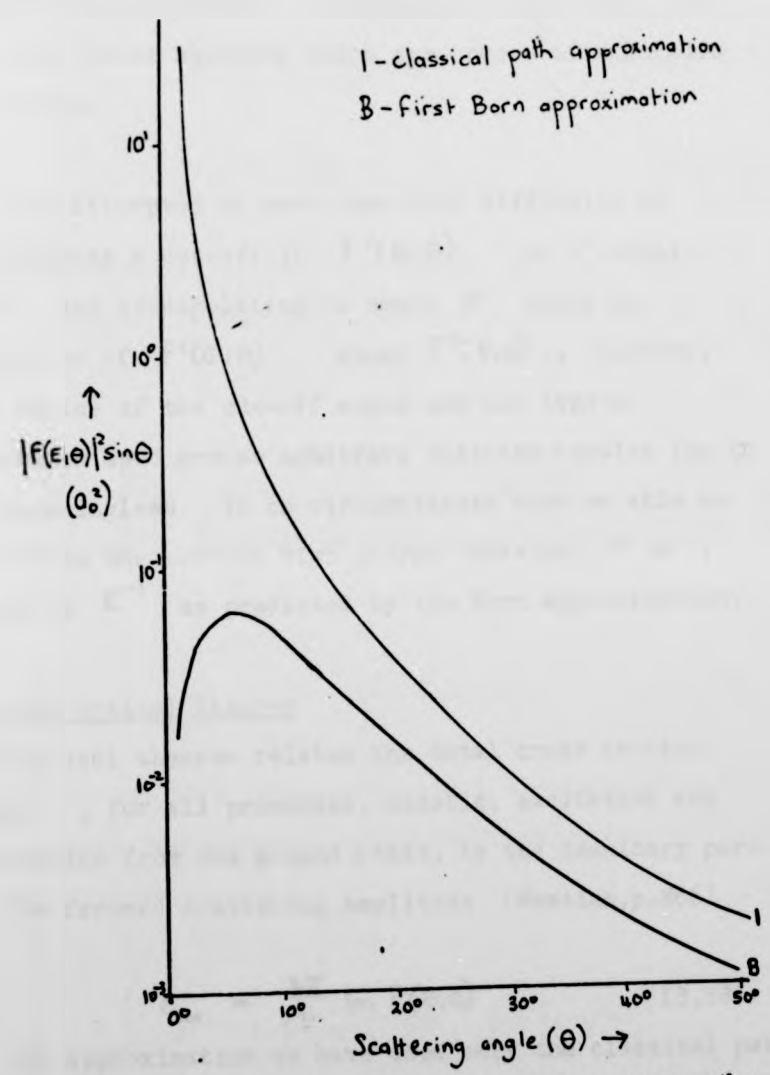(1973) will bear some relationship to this phenomena.

3.7 The Total Cross Section

The total cross section for elastic scattering is given by

$$\sigma = 2\pi \int_0^\pi |f(E,\theta)|^2 \sin\theta\, d\theta \qquad (3.57)$$

We shall investigate the use of the classical path
expression for the scattering amplitude in Equation (3.57).
An obvious difficulty arises at small scattering angles as
$|f^c(E,\theta)|^2$ is singular at $\theta = 0$. In Figure (3.13)
we have plotted the integrand $|f(E,\theta)|^2 \sin\theta$ as a
function of the scattering angle θ for both the Born
and the classical path approximations at $E = 1 kev$. Clearly

FIGURE 3.13

I - classical path approximation

B - First Born approximation

The distribution of the integrand $|F(\epsilon, \theta)|^2 \sin\theta$ with scattering angle θ.

Y-axis: $|F(\epsilon, \theta)|^2 \sin\theta$ (a_0^2), with values 10^1, 10^0, 10^{-1}, 10^{-2}, 10^{-3}

X-axis: Scattering angle $(\theta) \rightarrow$, with values $0°$, $10°$, $20°$, $30°$, $40°$, $50°$

there is a massive discrepancy at small angles. The
Born result for σ is generally believed to be
good because of the small angle behaviour
of the differential cross section in the Born
approximation. Therefore using the classical path
approximation $f^c(E,\theta)$ in Equation (3.57) will lead
to total cross sections which are orders of magnitude
too large.

We have attempted to over come this difficulty by
introducing a cut-off in $f^c(E,\theta)$ at a certain
θ , and extrapolating to small θ using an
expansion of $f^c(E,\theta)$ about $f^c(E,0)$. However,
the choice of the cut-off angle and the type of
expansion used are so arbitrary that the results for σ
are meaningless. In no circumstances were we able to
reproduce the correct high energy behaviour of σ ,
which is E^{-1} as predicted by the Born approximation.

b) The Optical Theorem

The optical theorem relates the total cross section,
σ_{tot} , for all processes, elastic, excitation and
ionisation from the ground state, to the imaginary part
of the forward scattering amplitude (Messiah,p.866)

$$\sigma_{tot} = \frac{4\pi}{q} \, \text{Im} \, F(E,0) \qquad (3.58)$$

In the approximation we have used only the classical path
term contains an imaginary part so we can express σ_{tot}

in terms of the imaginary part of the zero angle classical
path contribution to the scattering amplitude. From
Equations (3.43b) and (3.49b) we have

$$\sigma_{tot} = \frac{4\pi}{q_i^2} \left[256 \int_0^{E^{1/2}} \frac{dq \, q^2}{(1+q^2)^6 (1-\exp(-2\pi v_1))} \right.$$

$$\left. + \frac{12.8}{q_i^2} \int_0^{(2E)^{1/2}} \frac{q \, dq}{(\exp(2\pi v_2)-1)} \left\{ \frac{1}{[1+(q-q_i)^2]^5} - \frac{1}{[1+(q+q_i)^2]^5} \right\} \right] \tag{3.59}$$

where

$$v_1 = \frac{1}{\sqrt{E-q^2}} \tag{3.60a}$$

$$v_2 = \frac{2}{\sqrt{2E-q^2}} \tag{3.60b}$$

We are interested in the high energy limit of σ_{tot}.
In this limit $v_1 \to E^{-1/2}$ and the contribution to σ_{tot}
from the electron-proton interaction is given by

$$\sigma_{tot}^{(2)} \underset{E \to \infty}{=} \frac{4\pi}{q_i^2} \, 256 \, \frac{E^{1/2}}{2\pi} \int_0^\infty \frac{dq \, q^2}{(1+q^2)^6} \tag{3.61a}$$

The integral is obtained trivially and we obtain the
high energy limit

$$\sigma_{tot}^{(2)} \underset{E \to \infty}{=} 7\pi \tag{3.61b}$$

Similarly the high energy limit of the contribution to
the forward angle scattering amplitude from the
electron-electron paths is

$$\sigma_{tot}^{(3)} = \frac{4\pi}{q_i^2} \, \frac{12.8}{q_i^2} \, \frac{1}{2\pi} \, \frac{E^{1/2}}{2} \times$$

$$\times \int_0^\infty q \, dq \left[\frac{1}{\{1+(q-q_i)^2\}^5} - \frac{1}{\{1+(q+q_i)^2\}^5} \right] \tag{3.62a}$$

The integral, although more complicated than that for the
electron-proton interaction, can be evaluated by contour

integration and in the high energy limit gives the
result

$$\sigma_{tot}^{(3)} \underset{E \to \infty}{=} \frac{51\pi}{2^{7/2}} \tag{3.62b}$$

We therefore see that theory predicts that σ_{tot}
approaches a constant for $E \to \infty$. We have checked
Equations (3.61b) and (3.62b) numerically, and although
at the very high energies necessary for the asymptotic
value to be approached our programme loses accuracy, it
appears that the theoretical limits are approached and
that σ_{tot} decreases to these values at high energies.
The correct behaviour of σ_{tot} at asymptotic energies.
is given by the Bethe form (Mott and Massey, p.496)

$$\sigma_{tot} \underset{E \to \infty}{=} E^{-1}(A \log E + B)\pi \tag{3.63}$$

where A and B are constants. Therefore although the
first order Faddeev improves on the first order Born,
which gives $\sigma_{tot} = 0$ from the optical theorem, it does
not give the correct high energy behaviour. In the first
order Faddeev approximation three-body effects are
neglected and these will alter the behaviour of σ_{tot}
calculated from the optical theorem, when higher orders
of the Faddeev expansion are taken into account. Roberts
(1967) has shown that the imaginary part of the forward
scattering amplitude calculated in the second Born
approximation yields the optical theorem for the first
Born approximation. We therefore expect that calculations

of the second order Faddeev amplitude will vastly improve
predictions for σ_{tot} got from the optical theorem.

We note that the forward scattering amplitude can be
calculated directly from the spectral operator by
allowing $p \to p'$ in Equation (2.29). We have a
correspondence identity for the spectral operator
(Norcliffe et.al., 1969b) and therefore in principle

σ_{tot} can be expressed via the optical theorem
in terms of classical paths. The subjects of unitarity
of the Coulomb T matrix, the spectral operator and the
optical theorem are seen to be interelated to each other
and all dependent on classical trajectories.

CHAPTER 4

THE INELASTIC e-H SCATTERING PROBLEM

In this section we shall deal only with direct collisions,
a brief mention of rearrangement collisions will be made
in the final chapter. Equations (3.1), (3.2) and (3.4)
describing the scattering process, the scattering
amplitude and the conservation of energy respectively,
hold for the case of inelastic scattering with minor
modifications to some of the terms in the equations.
The initial and final energies E_i and E_f , and the
magnitudes of the asymptotic momenta q_i and q_f are
no longer equal for inelastic collisions, but must be
calculated from Equation (3.4) for each individual
process considered. The differential cross section is
given in terms of the scattering amplitude by (Mott and
Massey, p.475)

$$\frac{d\sigma}{d\Omega} = \frac{q_f}{q_i} \left| F(\epsilon,\theta) \right|^2 \qquad (4.1)$$

We shall deal only with the $n = 1 \to 2$ transition in
hydrogen. The $n = 2$ state of hydrogen has two substates
of the orbital quantum number l ; $l = 0$ known as the
$2s$ state and $l = 1$, the $2p$ state. The $2p$ state
is further subdivided into three levels characterised
by the magnetic quantum number m , which can take the
values $0, \pm 1$. Neglecting the spin-orbit and hyperfine
interactions the four $n = 2$ states are degenerate in

energy, the energy of this level being $E_2 = -p_0^2/8\mu_{23}$.
Thus the relationship between the initial and final
momenta is

$$\frac{q_i^2 - q_f^2}{2\mu_1} = \frac{3p_0^2}{8\mu_{23}} \qquad (4.2)$$

The transition amplitude is calculated in the first
order iterate of the Faddeev equations for each of the
transitions between the ground state and one of the four
excited substates. The total amplitude is just the sum
of the individual contributions.

We shall again concentrate our attention on the
contributions arising from the classical path term of
the two-body T matrix, and examine the cancellation
of the pole and Born terms only qualitatively. Much
of the analysis follows on from Chapter 3.

4.1 The Classical Path Terms

The coordinate relations in the barycentric frame for
the inelastic scattering process are the same as for
elastic scattering. We can write down the analogues of
Equations (3.11) and (3.14) by simply changing the final
state wave functions

$$\langle f|T_2(E)|i\rangle = \int dq_2 \, \phi_{2cm}^*(q_2) \, \phi_{1s}(q_2) \langle q_f|T_2(E-\frac{q_f^2}{2m_e})|q_i\rangle \quad (4.3a)$$

$$\langle f|T_3(E)|i\rangle = \int dq_3 \, \phi_{2cm}^*(q_3+q_f) \, \phi_{1s}(q_3+q_i) \langle q_f+\frac{q_3}{2}|T_3(E-\frac{q_3^2}{4m_e})|q_i+\frac{q_3}{2}\rangle \quad (4.3b)$$

where $\phi_{2cm}(q)$ is the final state wavefunction of the
bound system.

The definition of the two-body T matrices is dependent on the sign of $(\varepsilon - T)$ and $(\varepsilon - T')$. For both the electron-proton and the electron-electron interactions we can show that $T, T' > \varepsilon$ as for elastic scattering. We must therefore make the same choices for $g(T, T')$, that is, $g(T, T') = 1$ for the attractive interaction and $g(T, T') = \exp(-2\pi \vartheta)$ for repulsive scattering. Proceeding with the analysis as in Chapter 3 we obtain the following results for the matrix elements

$$\langle F|T_2(\varepsilon)|i \rangle = \frac{-4}{m_e \Delta q} \int\limits_{0<q<\varepsilon^{1/2}} \frac{dq \; \phi_{2em}^*(q) \, \phi_{1s}(q)}{(1/4+q^2)^{1/2}(1+q^2)^{1/2}(1+\frac{1}{2}z)^{1/2}} \; \frac{\exp(i\nu\omega)}{1-\exp(-2\pi\vartheta)} \quad (4.4)$$

where
$$z = \frac{2(\varepsilon - q^2)\Delta q^2}{(1+q^2)(1/4+q^2)} \quad (4.5)$$

and ω and ϑ are as defined in (3.22b,c).

$$\langle F|T_3(\varepsilon)|i \rangle = \frac{1}{2m_e \Delta q} \int\limits_{0<q_{23}<(2\varepsilon)^{1/2}} \frac{dq_3 \; \phi_{2em}^*(q_{23}) \, \phi_{1s}(q_{23})}{(q_{23}^2+1/4)^{1/2}(q_{23}'^2+1)^{1/2}(1+\frac{1}{2}z)^{1/2}} \; \frac{\exp(-i\nu\omega)\exp(-2\pi\vartheta)}{1-\exp(-2\pi\vartheta)} \quad (4.6)$$

where
$$z = \frac{2(2\varepsilon - q_3^2)\Delta q^2}{(q_{23}^2+1/4)(q_{23}'^2+1)} \quad (4.7)$$

ω and ϑ are defined in (3.26b) and (3.29), and q_{23}^2 and $q_{23}'^2$ we defined in Equations (3.31a,b). The momentum transfer Δq is given in atomic units by

$$\Delta q^2 = q_i^2 + q_f^2 - 2 q_i q_f \cos \theta \quad (4.8)$$

where from (4.2)

$$q_i^2 = q_f^2 + \frac{3}{4} \quad (4.9)$$

Equations (4.4) and (4.6) hold generally for all $n = 1 \to 2$
transitions. It only remains to consider specific
transitions and to insert into these equations the
relevant wave functions

a) $1s - 2s$ transition

The $2s$ state wavefunction of hydrogen in momentum
representation is

$$\phi_{200}(q) = \frac{1}{\pi} \frac{q^2 - 1/4}{(q^2 + 1/4)^3} \tag{4.10}$$

The wavefunction is independent of angle so we obtain
once again a single integral in the expression for the
electron-proton term and a triple integral for the
electron-electron term. The resulting contributions to
the scattering amplitude are

$$F_2^c(E, \theta) = \frac{32\sqrt{2}}{\Delta q} \int_0^{E^{1/2}} \frac{dq \; q^2 (q^2 - 1/4)}{(q^2 + 1/4)^{1/2} (q^2 + 1)^{5/2} (1 + 1/2^2)^{1/2}} \frac{\exp(iv\omega)}{1 - \exp(-2\pi\vartheta)} \tag{4.11}$$

$$F_3^c(E, \theta) = \frac{-4\sqrt{2}}{\Delta q} \int_{0 \Delta q_3 < (2E)^{1/2}} dq_3 \frac{q_3^2 - 1/4}{(q_{23}^2 + 1/4)^{1/2} (q_{23}^2 + 1)^{5/2} (1 + 1/2^2)^{1/2}} \frac{\exp(-iv\omega) \exp(-2\pi\vartheta)}{1 - \exp(-2\pi\vartheta)} \tag{4.12}$$

b) $1s - 2p$ transitions

The wavefunctions of the three sublevels of the $2p$
states of hydrogen are

$$m = 0 \quad ; \quad \phi_{210}(q) = \frac{1}{\pi} \frac{q}{(q^2 + 1/4)^3} \cos\theta \tag{4.13a}$$

$$m = \pm 1 \quad ; \quad \phi_{21\pm1}(q) = \frac{1}{\pi\sqrt{2}} \frac{q}{(q^2 + 1/4)^3} \sin\theta \; e^{\pm i\phi} \tag{4.13b}$$

The final state wave function is the only factor in
Equation (4.4) with angular dependence. On performing

the angular integration we find that for each value of m

$$\langle F|T_2(E)|i \rangle = 0 \qquad (4.14)$$

and hence the contribution to the scattering amplitude for the $1s-2p$ transition from the electron-proton interaction is zero.

Therefore the only contribution to the $1s-2p$ cross section is from the electron-electron paths. We have seen for elastic scattering that at large angles of scattering these paths contribute a negligible amount to the cross section and there is nothing different about the inelastic process which could alter this fact. We therefore expect that in this approximation the contributions to the $n=1 \to 2$ cross section from $1s-2p$ transitions will be underestimated, and for this reason we place less importance on our $1s-2p$ calculations than on the $1s-2s$ calculations.

We must take care in formulating the angular part of the electron-electron contribution to the $1s-2p$ transition amplitude. The angular integration in Equation (4.6) is over the vector q_3 whereas the final state wavefunction is defined by $q_{23} = q_3 + q_f$. We must relate the polar coordinates (θ', ϕ') of q_{23} to those, (θ, ϕ), of q_3 in order to simplify the integration. Figure (4.1) shows the orientations of q_3 , q_{23} and q_f , and on taking components of these vectors along the x, y and z axes we obtain the following coordinate relations
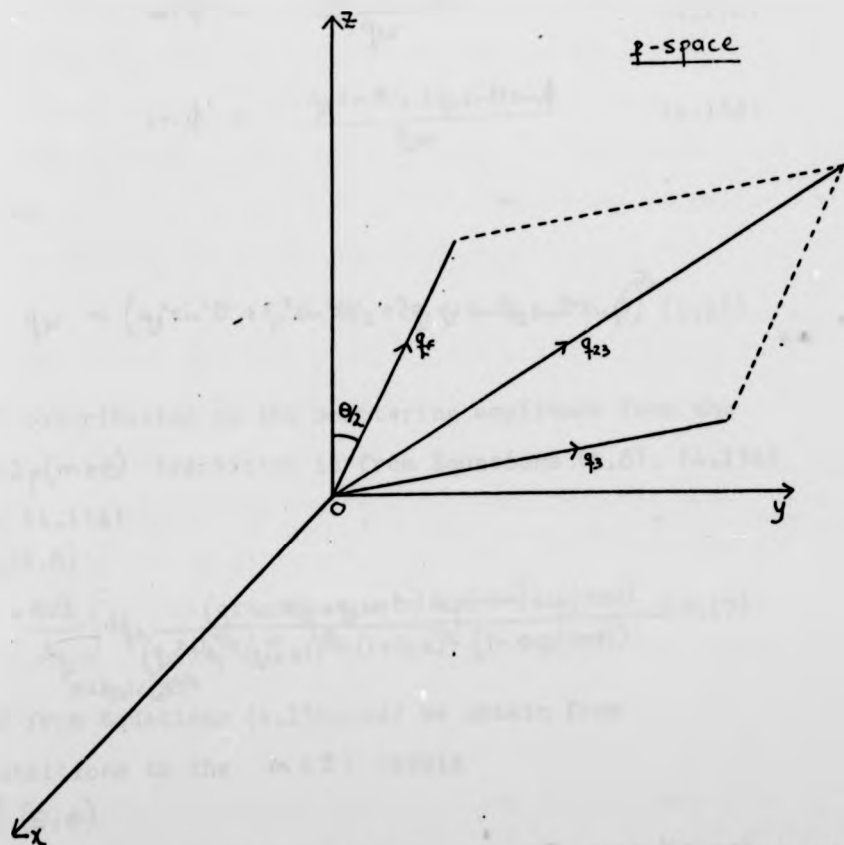
FIGURE 4.1

The orientation of the vectors q_3, q_F and $q_{23} = q_3 + q_F$.

q_3 has polar coordinates (q_3, θ, ϕ).

q_F has polar coordinates $(q_F, \theta/2, 0)$.

q_{23} has polar coordinates (q_{23}, θ', ϕ').

$$\cos \theta' = - \frac{q_F \cos \theta/2 + q_3 \cos \theta}{q_{23}} \qquad (4.15a)$$

$$\sin \theta' = \frac{q_{3F}}{q_{23}} \qquad (4.15b)$$

$$\cos \phi' = \frac{-q_3 \sin \theta \cos \phi}{q_{3F}} \qquad (4.15c)$$

$$\sin \phi' = \frac{-q_F \sin \theta/2 + q_3 \sin \theta \sin \phi}{q_{3F}} \qquad (4.15d)$$

where

$$q_{3F} = \left(q_3^2 \sin^2 \theta + q_F^2 \sin^2 \theta/2 + 2 q_3 q_F \sin \theta/2 \sin \theta \sin \phi \right)^{1/2} \qquad (4.16)$$

The contribution to the scattering amplitude from the $1s - 2p (m=0)$ transition is from Equations (4.6), (4.13a) and (4.15a)

$$F_{3,0}^c (E, \theta)$$
$$= - \frac{4\sqrt{2}}{\Delta q} \int_{0 < q_{23} < (2E)^{1/2}} dq_{23} \frac{(q_F \cos \theta/2 + q_3 \cos \theta) \exp(-i\nu\omega) \exp(-2\pi\nu)}{\left(q_{23}^2 + 1/4\right)^{1/2} \left(q_{23}'^2 + 1\right)^{5/2} \left(1 + 1/2 z\right)^{1/2} \left(1 - \exp(-2\pi\nu)\right)} \qquad (4.17)$$

and from Equations (4.15b,c,d) we obtain from transitions to the $m = \pm 1$ levels

$$F_{3,\pm 1}^c (E, \theta)$$
$$= \frac{4}{\pi \Delta q} \int dq_{23} \frac{q_{3F} \left[\cos (\nu\omega \pm \phi') - i \sin (\nu\omega \pm \phi') \right] \exp(-2\pi\nu)}{\left(q_{23}^2 + 1/4\right)^{1/2} \left(q_{23}'^2 + 1\right)^{5/2} \left(1 + 1/2 z\right)^{1/2} \left(1 - \exp(-2\pi\nu)\right)} \qquad (4.18)$$

4.2   The Pole and Born Terms

Insertion of the Born term of the two-body Coulomb T matrix into Equation (4.3a) for the electron-proton

matrix element leads to a zero contribution for all
final state wavefunctions $\phi_{2em}(q)$. The two-body
T matrix is independent of the variable of
integration, and the initial and final state wave-
functions are orthogonal in each case. The only
contribution to the scattering amplitude comes from
the electron-electron interaction, and we can assume
that these contributions will be small. We have
calculated analytically the Born term for the $1s-2s$
interaction, and found that it is equal to the result
achieved using the first Born approximation.

The pole terms are simply calculated and are similar in
form to the pole terms for elastic scattering, apart from
the slight modifications needed for inelastic scattering
which appeared in the analysis for the classical path
terms. In the $1s-2s$ transition there are contributions
from both the electron-proton and the electron-electron
interactions, but for $1s-2p$ transitions only the latter
term contributes.

The cancellation between the pole term and the Born term
is not so complete for the $1s-2s$ transition as for
elastic scattering. This is largely due to the zero
contribution from the electron-proton Born term. Thus
at an energy of 200ev and a scattering angle of 20°,
the differential cross section would be halved by
inclusion of the Born and pole terms rather than using

solely the classical path terms. However, at a scattering angle of 60° the effect of these two terms is negligible, and at high energies, for instance, 1500ev, their effect is small for scattering angles above 20°.

Can we say that the on-shell correspondence identity holds for the $1s-2s$ transition? For small scattering angles we would not expect the identity to be true. For low energies (~ 200ev) in the energy range considered we have seen that the identity is not satisfied as closely as for elastic scattering, though within an order of magnitude the approximation is good. For higher energies the correspondence identity is satisfied over the whole angular range considered. With these reservations we shall apply the classical path terms in the Faddeev equations to calculate differential cross sections for energies above 200ev and scattering angles greater than 20°.

For $1s-2p$ transitions we have already stated that the contributions from the Born, pole and classical path terms are likely to be insignificant in comparison with the $1s-2s$ contributions to the scattering amplitude. Other than attempting to explain this phenomena physically, we shall neglect all contributions from the $1s-2p$ transition, so that the rest of this chapter will in the main be concerned with the $1s-2s$ transition.

4.3 Results and Discussion

Equations (4.11), (4.12), (4.17) and (4.18) have been
solved numerically using the computational techniques
described in the section on elastic scattering. The
electron-electron terms, for both the $1s-2s$ and the
$1s-2p$ transitions, are found to be numerically
insignificant in comparison with the electron-proton
term for the $1s-2s$ transition. The following results
are calculated from the latter term which is the sole
contribution of significance in the classical path
approximation. In figures (4.2) and (4.3) we present
the angular distributions of the differential cross
section at two incident particle energies; comparisons
are made with the Born and the Coulomb projected Born
(Geltman and Hidalgo, 1971 , hereafter referred to as
CPB) results.

It is immediately apparent that the angular behaviour
of the Born differential cross section is very different
from the similar behaviour predicted by the other two
theories. This is a result of the artificial cancellation
of the electron-proton interaction in the first Born
approximation. As stated in Chapter 3, large angle
scatterings are caused by the incident particle passing
close to the nucleus, in which case the electron-electron
contribution to the cross section is small. This explains
why the Born approximation gives reasonable results for
small angles of scattering, but underestimates the cross
section greatly at angles above 60°.
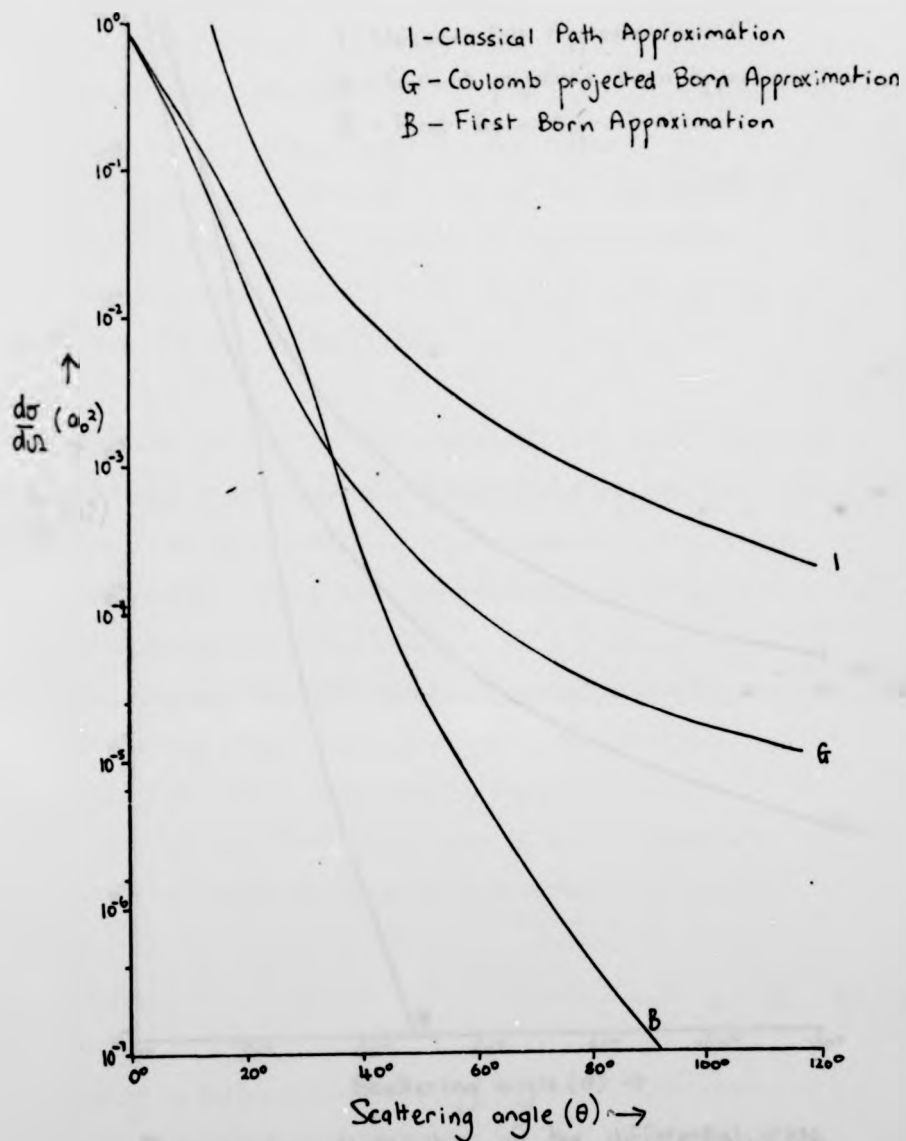
FIGURE 4.2

I - Classical Path Approximation
G - Coulomb projected Born Approximation
B - First Born Approximation

The angular distribution of the differential cross section for the collision $e^- + H(1s) \rightarrow e^- + H(2s)$ at incident energy 200 ev.

FIGURE 4.3

I — Classical Path Approximation
G — Coulomb projected Born Approximation
B — First Born Approximation
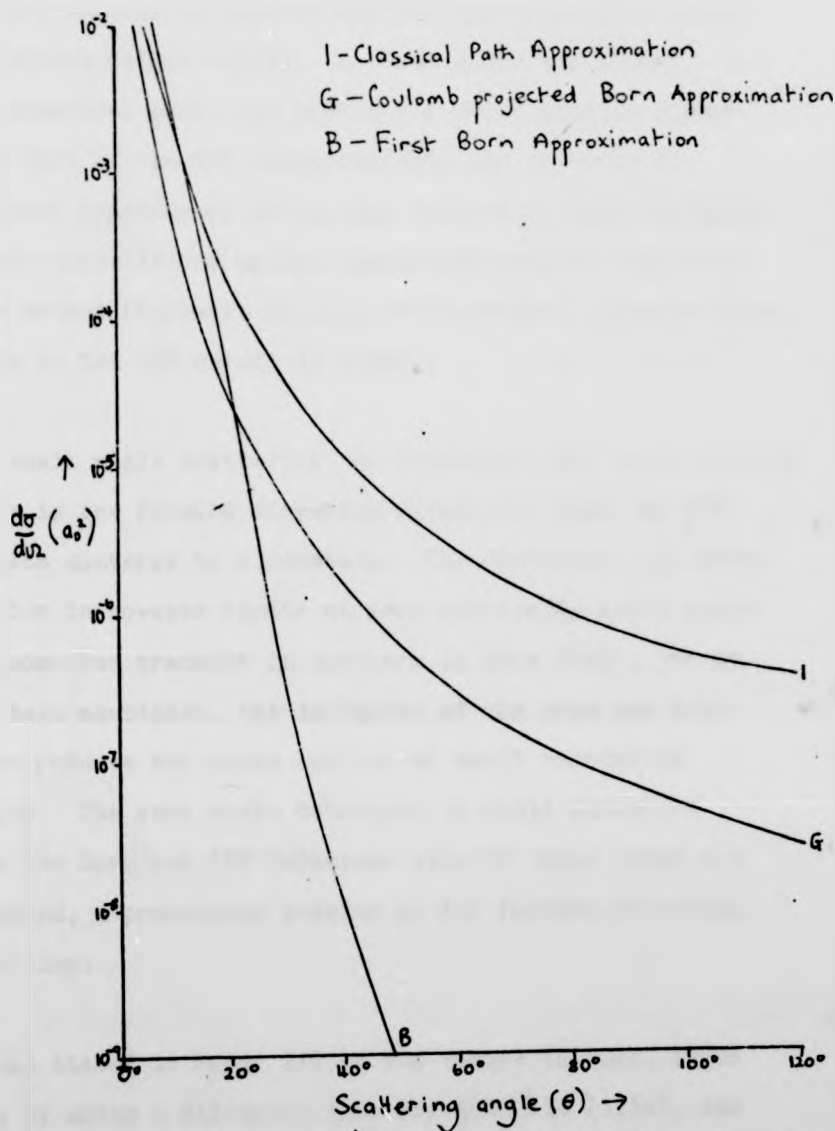
The angular distribution of the differential cross section for the collision $e^- + H(1s) \rightarrow e^- + H(2s)$ at incident energy 1500 ev.

Although at large angles of scattering the angular
distribution of the classical path term cross section
is very similar to that of the CPB approximation, their
magnitudes differ widely. At both 200ev and 1500ev
the classical path term predicts a cross section higher
than that of the CPB approximation, and there is no
apparent convergence of the two results at high energies.
Recent calculations using a polarised orbital distorted
wave method (McDowell et.al., 1973) predict cross sections
close to the CPB result at 200ev.

For small angle scattering the classical path cross section
peaks in the forward direction whilst the Born and CPB
results converge to a constant. The classical path cross
section is however finite at zero scattering angle since
the momentum transfer is non-zero in this limit, and as
has been mentioned, the inclusion of the pole and Born
terms reduces the cross section at small scattering
angles. The zero angle behaviour is still different
from the Born and CPB behaviour even if these terms are
included, a pronounced peaking in the forward direction
resulting.

It was stated in Paper III of the series (Hutton, 1972)
that by using a different form for $\mathfrak{z}(\tau,\tau')$ in (4.3a), one
obtains a differential cross section closer in magnitude
to the CPB result. This choice of $\mathfrak{z}(\tau,\tau')$ is arbitory
and as for elastic scattering we reiterate that a unique
definition of $\mathfrak{z}(\tau\tau')$ leads to the correct result given
by Equation (4.11).

We have already stated that the $1s-2p$ differential
cross section contributes a negligible amount to the
$n = 1 \rightarrow 2$ cross section. Taking the results
presented in Figure (4.2) to be the $n=1\rightarrow2$ cross section
at 200ev, our value is still an order of magnitude higher
than the CPB result, though the angular distributions
are almost identical at large scattering angles. The
experimental results quoted by Geltman and Hidalgo
(Williams, 1969) are normalised to the CPB approximation,
so that the magnitude of the differential cross section
is not definite.

For a fixed scattering angle the energy dependence of
the differential cross section using the CPB approximation
is E^{-3} , whereas the Born result goes asymptotically as
E^{-6} for $1s-2s$ excitation and E^{-7} for $1s-2p$. We have
supposed that the classical path approximation has the
asymptotic energy dependence

$$\frac{d\sigma}{d\Omega} \underset{E \to \infty}{=} \alpha(\theta) E^{-n} \qquad (4.19)$$

and have plotted $\log\left(\frac{d\sigma}{d\Omega}\right)$ against $\log E$ for several fixed
values of the scattering angle. A typical result is
shown in Figure (4.4) for $\theta = 90°$. Deviation from the
correct straight line behaviour is only apparent at
$E < 500ev$. The value of n is given by the gradient
of the line, and in Figure (4.5) we tabulate the values
of n obtained at different scattering angles. Within
the error involved in measuring the gradient, we see that
n lies between 3.1 and 3.2, and no regular dependence
on the scattering angle is apparent. The behaviour of

We have already stated that the $1s-2p$ differential cross section contributes a negligible amount to the $n = 1 \rightarrow 2$ cross section. Taking the results presented in Figure (4.2) to be the $n=1\rightarrow2$ cross section at 200ev, our value is still an order of magnitude higher than the CPB result, though the angular distributions are almost identical at large scattering angles. The experimental results quoted by Geltman and Hidalgo (Williams, 1969) are normalised to the CPB approximation, so that the magnitude of the differential cross section is not definite.
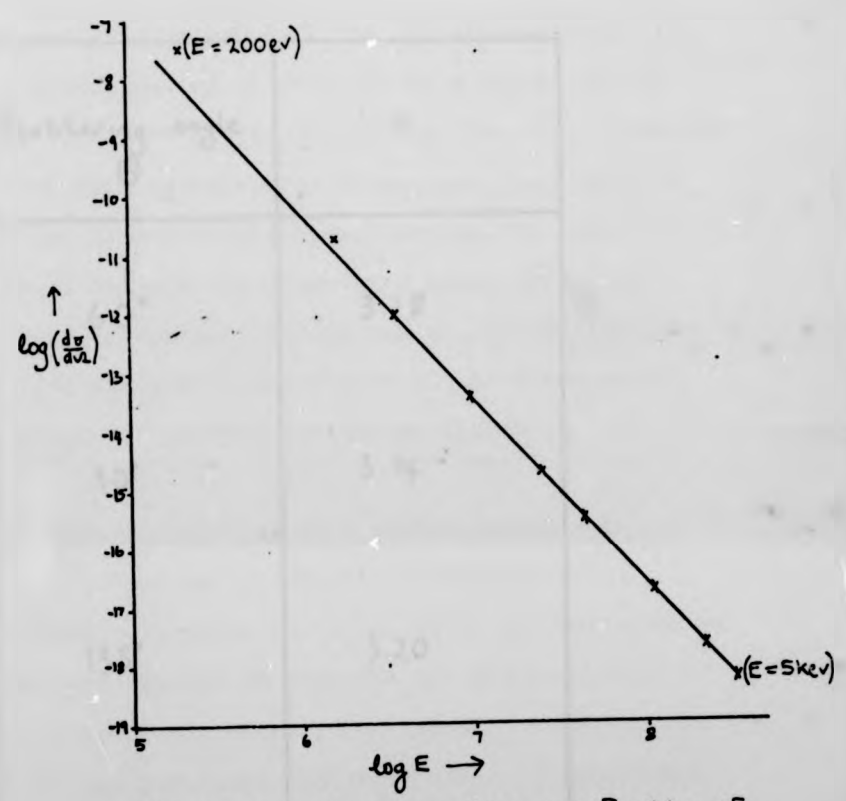
For a fixed scattering angle the energy dependence of the differential cross section using the CPB approximation is E^{-3}, whereas the Born result goes asymptotically as E^{-6} for $1s-2s$ excitation and E^{-7} for $1s-2p$. We have supposed that the classical path approximation has the asymptotic energy dependence

$$\frac{d\sigma}{d\Omega} \underset{E\to 0}{=} \alpha(\theta) E^{-n} \tag{4.19}$$

and have plotted $\log\left(\frac{d\sigma}{d\Omega}\right)$ against $\log E$ for several fixed values of the scattering angle. A typical result is shown in Figure (4.4) for $\theta = 90°$. Deviation from the correct straight line behaviour is only apparent at $E < 500$ev. The value of n is given by the gradient of the line, and in Figure (4.5) we tabulate the values of n obtained at different scattering angles. Within the error involved in measuring the gradient, we see that n lies between 3.1 and 3.2, and no regular dependence on the scattering angle is apparent. The behaviour of

FIGURE 4.4

The differential cross section as a function of energy on a log scale. From the equation $\frac{d\sigma}{d\Omega} = \alpha(\theta) E^{-n}$, the gradient of the line is n. In this case $\theta = 90°$, $n = 3.13$.

FIGURE 4.5

Scattering angle θ	n
60°	3.18
90°	3.14
135°	3.20
180°	3.18

The behaviour of $d\sigma/d\Omega$ as a function of energy at four fixed scattering angles.

$$\frac{d\sigma}{d\Omega} = \alpha(\theta) E^{-n}.$$

the differential cross section at high energies is
therefore very close to the CPB approximation behaviour,
and confirms the discrepancy between the latter and the
Born result.

This result is particularly important. The different
limiting energy dependence of the CPB approximation and
the Born approximation is shown to be a result of the
classical path part of the T matrix. The E^{-6} behaviour
of the Born term is cancelled by an equal but opposite
contribution from the pole term, leaving the classical
path term to dictate the asymptotic energy behaviour.
Experimental investigations are needed to establish the
correct limiting energy dependence of the differential
cross section at non-zero scattering angles.

4.4 The Coulomb projected Born approximation

This approximation was originally formulated for
rearrangement collisions (Geltman, 1971) and was modified
by Geltman and Hidalgo to describe the excitation of
hydrogen atoms by electrons. The transition amplitude
between initial and final states is given in coordinate
representation by

$$T_{if} = \left\langle \tilde{\psi}_f(r_1,r_2) \left| \frac{e^2}{|r_1 - r_2|} \right| \exp(i\underline{k}\cdot\underline{r}_1)\, \phi_i(r_2) \right\rangle \qquad (4.20)$$

Here the incident and bound electron coordinates are
given respectively by $\underline{r}_1$ and $\underline{r}_2$ with respect to the
proton which is considered fixed at the origin. $\tilde{\psi}_f(r_1,r_2)$
is the solution of the scattering problem obtained if one
ignores the electron-electron contribution $\frac{e^2}{|r_1 - r_2|}$)

and $\exp(i q_i \cdot r_i) \, \phi_i(r_2)$ is the initial wave function
for the electron and atom at infinite separation.
Essentially the CPB approximation evaluates the matrix
element of the repulsive interaction, and allows for the
distortion effect of the electron-proton interaction by
including it in the final state wave function. By doing
this the CPB approximation avoids the incorrect sharp
decrease of the differential cross section at intermediate
scattering angles predicted by the first Born approximation.

We have transformed the CPB approximation for excitation
into the barycentric momentum representation and obtained
the following expression for the scattering amplitude.

$$f^{CPB}(E, \theta) = G \times$$

$$\times \int dq_1 \, dq_{23} \, \frac{\phi_F^*(q_{23}) \, \phi_i(q_{23} + q_1 - q_i)}{(q_1 - q_i)^2 (q_1 - q_F)^2 (q_1^2 - q_F^2)} \left[1 + \frac{2 q_F \cdot (q_F - q_1)}{q_1^2 - q_F^2} \right]^{-i\alpha} \quad (4.21)$$

where G is the constant $\frac{m_e e^2}{\pi^3} \left(\frac{1}{2\pi} \right)^{1/2} \exp(-\tfrac{1}{2} \pi \alpha) \, \Gamma(1 + i\alpha) \, \alpha q_F$
and α is the Coulomb interaction parameter $-e^2 m_e / q_F$.
The scattering amplitude in the first order Faddeev
approximation involves a sum of two terms, both of
which are single integrals over a momentum vector.
In the CPB approximation $f^{CPB}(E, \theta)$ is an
integral over two momentum vectors, but is a single
term. This difference in the expressions for the
scattering amplitude makes a formal comparison of the
two theories difficult, however there are certain
similarities which we note below.

At high energies the Coulomb factor $\alpha = -\nu$. On making the identification

$$1 + \frac{2q_f \cdot (q_f - q_i)}{q_i^2 - q_f^2} = 1 + z' = \cosh \omega' \qquad (4.22)$$

we obtain in the integrand a factor

$$e^{i\nu\omega'}\left[1 + i\nu e^{-2\omega'} + \frac{i\nu(i\nu-1)}{2!} e^{-4\omega'} + \cdots\right] \qquad (4.23)$$

We cannot identify z' and ω' with z and ω , but can see that factors similar to the classical path term and the pole terms do appear in Equation (4.23). The fact that these terms cannot be separated out in the CPB approximation, is probably due to the mixing of momentum coordinates inherent in the double integral of Equation (4.21). The similar angular distributions of the CFB and Faddeev cross sections for inelastic scattering suggest that a formal comparison of the two theories may be possible, and further research along these lines would be profitable.

4.5 Concluding Remarks

We mention briefly here three phenomena which merit further investigation. Firstly that at high energies the electron-proton classical path contribution to the $1s-2s$ differential cross section tends to zero. It thus paradoxically appears to approach the Born result in the high energy limit. We have been unable to show analytically that the electron-electron classical path contribution approaches the corresponding Born term at high energies, but it appears numerically that this may

At high energies the Coulomb factor $\alpha = -\nu$. On making the identification

$$1 + \frac{2q_f \cdot (q_f - q_i)}{q_i^2 - q_f^2} = 1 + z' = \cosh \omega' \qquad (4.22)$$

we obtain in the integrand a factor

$$e^{i\nu\omega'}\left[1 + i\nu\, e^{-2\omega'} + \frac{i\nu(i\nu-1)}{2!}\, e^{-4\omega'} + \cdots\right] \qquad (4.23)$$

We cannot identify z' and ω' with z and ω , but can see that factors similar to the classical path term and the pole terms do appear in Equation (4.23). The fact that these terms cannot be separated out in the CPB approximation, is probably due to the mixing of momentum coordinates inherent in the double integral of Equation (4.21). The similar angular distributions of the CPB and Faddeev cross sections for inelastic scattering suggest that a formal comparison of the two theories may be possible, and further research along these lines would be profitable.

4.5 Concluding Remarks

We mention briefly here three phenomena which merit further investigation. Firstly that at high energies the electron-proton classical path contribution to the $1s-2s$ differential cross section tends to zero. It thus paradoxically appears to approach the Born result in the high energy limit. We have been unable to show analytically that the electron-electron classical path contribution approaches the corresponding Born term at high energies, but it appears numerically that this may

be the case. It would be strange if in the Faddeev formalism the same error appeared which makes the Born approximation unreliable for the calculation of differential cross sections, at large scattering angles, for inelastic scattering.

Secondly, and related to the latter phenomena, we consider the effect on the calculations of allowing the proton mass to be finite. The scattering process then needs a different description though many of the results are unchanged. Chen (1971) and ourselves have shown independently that the effect of a finite mass proton on elastic scattering calculations is to alter the asymptotic energy dependence of the differential cross section from E^{-2} to E^{-6}. The proton, which is now free to move, absorbs recoil energy, thereby accelerating the decrease of the differential cross section with respect to energy.

More importantly for inelastic scattering, the inclusion of a finite mass proton in the theory would mean that the electron-proton contribution to the Born term for the $1s-2s$ transition, to the high energy limit of the classical path approximation for the $1s-2s$ transition, and to the $1s-2p$ transition were all no longer zero. The infinite mass approximation is good for elastic scattering and $1s-2s$ excitation, but for the $1s-2p$ transition when the electron-electron interactions are small, the inclusion of the finite mass of the proton would significantly alter the results.

Finally, having shown that the differential cross section is finite at small angles for inelastic scattering, we ask whether we can predict correct total cross sections. The classical path calculation of the differential cross section is strongly peaked for forward scattering, and therefore the integrated cross section is overestimated. if calculated from this term alone. By including all three parts of the Coulomb T matrix one may in principle be able to predict the correct zero angle behaviour, in which case the integrated cross section would also be correct. However, there still remains the apparent over estimation of the differential cross section by the first order iterate of the Faddeev equations, an effect which it appears can be overcome by including second order terms (Chen et.al., 1973). We therefore assume that the first order iterate of the Faddeev equations is insufficiently accurate to predict correct total cross sections.

CHAPTER 5

CONCLUDING REMARKS

5.1 Rearrangement Collisions

Controversy over the correct limiting energy dependence
of the total cross section for electron exchange
processes such as proton impact on hydrogen atoms has
existed for many years. In a review article,
(Bransden, 1965), it is demonstrated that even within
the first Born approximation ambiguities exist as
to what is the correct energy behaviour. Brinkman
and Kramers (1930) argued that the internuclear
potential should not contribute to the cross section
to order m_e/m_p where m_p is the mass of the proton. Bates
and Dalgarno (1952) included the internuclear potential
in their calculations and found that the limiting
energy dependence of this term was equal to that of
the Brinkman-Kramers term and its effect was to reduce
the cross section by one third. The second Born
calculation of Drisko (1955) indicated a different
asymptotic limit altogether from the first Born
approximation.

It was thus hoped that the Faddeev approach would resolve
these ambiguities inherent in the Born approximation.
In the Faddeev equations occurred the two-body off-shell
T matrix for the proton-proton interaction, and it
was reasonably hoped that this term would be considerably
smaller than the bare potential term. Bransden has

shown that at high energies the scattering is confined
almost entirely to the forward direction. We have
shown for direct collisions that the classical path
term of the T matrix is of no use for predicting
differential cross sections at small angles of
scattering. The use of this term in the Faddeev
equations for rearrangement collisions is therefore
ruled out.

Chen (1972) has reviewed the work of his group on
rearrangement collisions. It appears that in the
first order iterate of the Faddeev equations the limiting
energy behaviour of the cross section lies between the
Brinkman-Kramer and Bates-Dalgarno results. Furthermore
it is shown that the second order terms of the Faddeev
equations make significant contributions to the cross
section, though all of these contributions are not
evaluated. The Faddeev equations have up till now
failed to resolve the ambiguities in the limiting
energy dependence of the total cross section for
rearrangement collisions.

5.2 The Faddeev Equations

We have applied the first order iterate of the Faddeev
equations to both elastic and inelastic collisions at
high energies. Comparison between our results and those
of Chen and Sinfailan (1972) for the elastic differential
cross section at energies above 200ev and scattering
angles above 30°, show that the classical path

approximation to the T matrix is good. It therefore
appears that for elastic scattering the first order
Faddeev and Born approximations make considerably
different predictions for the magnitude of the
differential cross section. Convergence of the
two results is only apparent at energies an order of
magnitude greater than that energy at which the Born
approximation is expected to be accurate. Experimental
investigations tentatively suggest that the differential
cross section is overestimated in the first order
Faddeev approximation. For inelastic scattering the
predictions of the Faddeev method improve on the Born,
in that the incorrect rapid decrease of the differential
cross section with angle is avoided. The Faddeev
differential cross section is greater in magnitude than
that predicted by the Coulomb projected Born result
(Geltman and Hidalgo, 1971), though the angular and
energy distributions of the two theories are very close.

As has been mentioned recent investigations of the
second order term of the Faddeev expansion by Chen
et.al. (1973) have suggested that there are important
contributions to the differential cross section from this term.
The second order iterate of the Faddeev equations has
been evaluated in the eikonal approximation using the
angle approximation for the classical trajectories
(Chen and Watson, 1969). Singularities appearing in
the calculations for the first and second order terms

of the series cancel when the terms are summed. These
singularities are associated with the difficulties
involved in taking the on-shell limit of the Coulomb
T matrix. In the second order iterate of the Faddeev
equations for elastic scattering at 200 ev, the
differential cross section calculated in this way
is very close to the prediction of the first order
Born approximation. We conclude therefore that the
differential cross section for direct collision
processes is overestimated by the first order iterate
of the Faddeev equations.

5.3 The Coulomb T Matrix and the Significance of the Correspondence Identities

Due to the long range nature of the Coulomb potential
singularities appear in the on-shell limit of the
two-body off-shell Coulomb T matrix. These singularities
lead to factors in the differential cross section which
are responsible for the difficulties mentioned in
Section (5.2). The ambiguities in the definition of
the differential cross section due to these factors
referred to in the literature (Hutton and Roberts,1972,
Hutton 1972) have been removed. Singularities in the
Coulomb T matrix also appear at zero scattering angles
for elastic scattering, and these lead to a small angle
divergence of the differential cross section.

The on-shell correspondence identity for the Coulomb
T matrix (Roberts, 1971b) is shown to provide a good

approximation when used to describe scattering phenomena at energies above 200ev and scattering angles above 30°. Outside of this region quantal effects are important in the form of the Born and pole terms of the Coulomb T matrix. The correspondence identity is related to the correspondence identity for the spectral operator (Norcliffe et.al. 1969b) so the latter is also shown to stand up to a physical test. Classical considerations associated with these correspondence identities have been shown to contribute to the explanation of

i) the slow high energy convergence of the Born and Faddeev differential cross sections for elastic scattering.

ii) the differing energy dependences of the differential cross section for inelastic scattering predicted by the Born and Coulomb projected Born theories.

Thus, despite the reservations about the application of the first order iterate of the Faddeev equations, the classical path approximation is shown to be a useful method, reducing the complication of calculations at high energies and giving insight into the physics of direct atomic collision processes.

APPENDIX

Calculation of the electron-electron part of the Born T-matrix contribution to the elastic scattering amplitude

We need to evaluate

$$\langle F | T_3^\theta(E) | i \rangle = \frac{p_c}{2\pi^2 \mu_{12} \Delta q^2} \int dq_{23} \, \phi_{1s}^*(q_3 + q_F) \, \phi_{1s}(q_3 + q_i) \quad (A.1)$$

It is convenient to transform to the dummy vector $\underline{x}$ given by

$$\underline{x} = q_{23} = q_3 + q_F \quad (A.2)$$

then (A.1) can be written

$$\langle F | T_3^\theta(E) | i \rangle = \frac{p_o}{2\pi^3 m_e \Delta q^2} \int d\underline{x} \, \phi_{1s}^*(\underline{x}) \, \phi_{1s}(\underline{x} + \Delta q) \quad (A.3)$$

Inserting the expression for the momentum space wave functions given by Equation (3.20) and performing the trivial angular part of the integration, we obtain in atomic units

$$\langle F | T_3^\theta(E) | i \rangle = \frac{4}{\pi^3 m_e \Delta q^3} \int_0^\infty \frac{dx \, x}{(x^2 + 1)^2} \times$$
$$\times \left[\frac{1}{1 + (x - \Delta q)^2} - \frac{1}{1 + (x + \Delta q)^2} \right] \quad (A.4)$$

The integrand is even so we can write

$$\int_0^\infty dx \, x \cdots = \frac{1}{2} \int_{-\infty}^\infty dx \, x \cdots \quad (A.5)$$

Consider integrating the function $F(z)$ around the contour C shown in Figure (A.1) where

$$F(z) = \frac{z}{(z^2+1)^2\left[1+(z-\Delta q)^2\right]}$$

The function $F(z)$ has poles inside C at $z=i$ of order 2, and at $z=i+\Delta q$ of order 1. The residues are simply calculated by reference to Spiegel (p.172)

$$R(i) = \frac{i(i-\Delta q)}{2\left[(i-\Delta q)^2+1\right]^2} \qquad (A.6a)$$

and

$$R(i+\Delta q) = \frac{-i}{2}\frac{i+\Delta q}{\left[1+(i-\Delta q)^2\right]^2} \qquad (A.6b)$$

where $R(i)$ is the residue of the pole at $z=i$

Similarly we integrate the function $g(z)$ around C where

$$g(z) = \frac{z}{(z^2+1)^2\left[1+(z+\Delta q)^2\right]} \qquad (A.7)$$

and $g(z)$ has poles at $z=i$ of order 2, and at $z=i-\Delta q$ of order 1, both lying inside C. The residues of these poles are given by
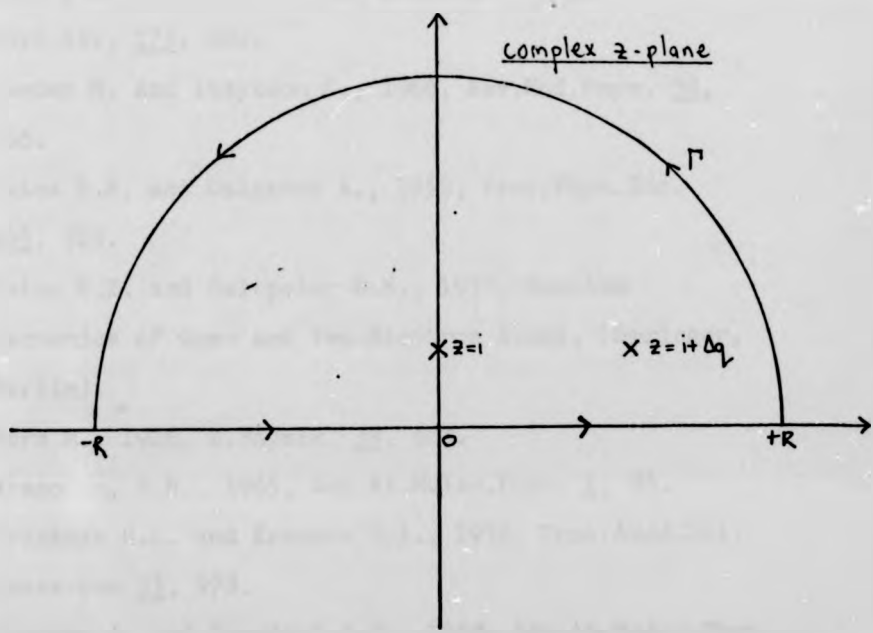
$$R(i) = \frac{-i(i+\Delta q)}{2\left[(i+\Delta q)^2+1\right]^2} \qquad (A.8a)$$

$$R(i-\Delta q) = \frac{i(i-\Delta q)}{2\left[(i-\Delta q)^2+1\right]^2} \qquad (A.8b)$$

Now letting $R\to\infty$ and noting that the contribution from the curved part of the contour C tends to zero in this limit (Spiegel, p.174) we have using the residue theorem

$$\langle F|T_3^\beta(\epsilon)|i\rangle = \frac{8}{\pi^2 m_e \Delta q^2 (\Delta q^2+4)^2} \qquad (A.9)$$

B.R.

FIGURE A1: THE CONTOUR C

complex z-plane

$$f(z) = \frac{z}{(z^2+1)^2[1+(z-\Delta q)^2]}$$

x indicates poles of $f(z) = \dfrac{z}{(z^2+1)^2[1+(z-\Delta q)^2]}$ lying within C.

REFERENCES

Aaron R., Amado R.D. and Lee B.W., 1961, Phys.Rev. 121, 319.

Ahmazadeh, A. and Tjon J.A., 1965, Phys.Rev. 139, B1058.

Ball J.S., Chen J.C.Y. and Wong,D.Y., 1968, Phys.Rev. 173, 202.

Bander M. and Itzykson C., 1966, Rev.Mod.Phys. 38, 346.

Bates D.R. and Dalgarno A., 1952, Proc.Phys.Soc. A65, 919.

Bethe H.E. and Saltpeter E.E., 1957, Quantum Mechanics of One- and Two-Electron Atoms, (Springer, Berlin).

Born M., 1926, Z.Physik 38, 803.

Bransden, B.H., 1965, Adv.At.Molec.Phys. 1, 85.

Brinkman H.C. and Kramers H.A., 1930, Proc.Acad.Sci. Amsterdam 33, 973.

Burgess A. and Percival I.C., 1968, Adv.At.Molec.Phys. 4, 109.

Burke P.G. and Seaton M.J., 1971, Methods in Comp.Phys. 10, 1.

Chen J.C.Y., 1972, Progress Reports Physics of Electronic and Atomic Collisions VII ICPEAC 1971, (North Holland, Amsterdam).

Chen J.C.Y. and Chen A.C., 1972, Adv.At.Molec.Phys. 8, 72.

Chen J.C.Y., Chen A.C., Sinfailam A.-L. and Hambro L., 1971, Phys.Rev. A4, 1998.

Chen J.C.Y., Chung K.T. and Kramer P.J., 1969,
Phys.Rev. 184, 64.

Chen J.C.Y., Hambro L., Sinfailam A.-L., and
Chung K.T., 1973, Phys.Rev. A7, 2003.

Chen J.C.Y. and Joachain C.J., 1971, Physica 53, 333.

Chen J.C.Y. and Sinfailam A.-L., 1972, Phys.Rev.A5, 1218.

Chen J.C.Y. and Watson K.M., 1969, Phys.Rev. 183, 236.

Dettmann K. and Leibfried G., 1968, Z.Physik 210, 43.

Drisko, R.M., 1955, Thesis Carnegie Inst.of Tech.

Faddeev L.D., 1961, Sov.Phys. - JETP 12, 1014.

Faddeev, L.D., 1961, Sov.Phys. - DOK 6, 384.

Faddeev, L.D., 1963, Sov.Phys. - DOK 7, 600.

Faddeev L.D., 1965, Mathematical Aspects of the
Three-Body Problem in the Quantum Scattering Theory,
(The Israel Program for Scientific Translations,
Jerusalem).

Faddeev L.D., 1970, Proc.1st.Int.Conf. on Three-Body
Problem in Nuclear and Particle Physics, (North
Holland, Amsterdam).

Fock, V.A., 1935, Z.Physik 98, 145.

Ford W.F., 1964, Phys.Rev. 133B, 1616.

Geltman S., J. Phys. B: Atom.Molec.Phys. 4, 1288.

Geltman S., and Hidalgo M.B., 1971, J.Phys.B: Atom.
Molec.Phys. 4, 1299.

Goldberger M.L. and Watson K.M., 1964, Collision Theory,
(McGraw-Hill, New York).

Hostler L., 1964, J.Math.Phys. 5, 591.

Hutton, N.A., 1972, J.Phys.B: Atom.Molec.Phys. 5,L246.

Hutton N.A. and Roberts M.J., 1972, J.Phys.B: Atom.
Molec.Phys. 5, L104.

Lippman B., and Schwinger J., 1950, Phys. Rev. 91,469.

McDowell M.R.C., Morgan L.A. and Myerscough V.P.,
1973, J.Phys.B: Atom.Molec.Phys. 6, 1435.

Messiah A., 1965, Quantum Mechanics Vol. 2,
(North Holland, Amsterdam).

Mott N.F. and Massey, H.S.W., 1965, The Theory of
Atomic Collisions, (Oxford, London).

Newton R.G., 1966, Scattering Theory of Waves and
Particles, (McGraw Hill, New York).

Norcliffe A., Percival I.C. and Roberts M.J., 1969a,
J.Phys.B: Atom.Molec.Phys. 2, 578.

Norcliffe A., Percival I.C. and Roberts M.J., 1969b,
J.Phys.B:Atom.Molec.Phys. 2, 590.

Nuttall J. and Stagat R.W., 1971, Phys.Rev. A3, 1355.

Okubo S. and Feldman D., 1960, Phys.Rev. 117, 292.

Perelemov A.M. and Popov V.S., 1966, Sov.Phys. -
JETP 23, 118.

Roberts M.J.. 1967, Proc.Phys.Soc. 91, 508.

Roberts M.J., 1970a, Chem.Phys.Lett. 6, 46.

Roberts M.J., 1970b, J.Phys.B: Atom.Molec.Phys. 3, L115.

Schwinger J., 1964, J.Math.Phys. 5, 1606.

Shastry, C.S., Rajagopal A.K. and Callaway J., 1972,
Phys.Rev. A6, 268.

Spiegel M.R., 1964, Complex Variables, (McGraw Hill,
New York).

Tai H., Teubner P.J. and Bassel, R.H., 1969, Phys.
Rev.Lett. 22, 1415.

Teubner P.J.O., Lloyd C.R. and Weigold E., 1973,
J.Phys.B: Atom.Molec.Phys. 6, L134.

Teubner P.J.O., Lloyd C.R., Weigold E. and Lewis,B.R.,
1973, Abstr. VIII Int.Conf.on Physics of Electronic
and Atomic Collisions (Institute of Physics, Belgrade),
259.

Williams, K.G., 1969, Abstr.VI Int.Conf. on Physics
of Electronic and Atomic Collisions,(M.I.T. Press,
Cambridge Mass.), 731.

Zemach Ch. and Klein A., 1958, NUOVO CIMENTA $\underline{10}$, 1078.